Analysis of the statistics of sandpile avalanches using soil-mechanics results and concepts

Pierre Evesque*
Laboratoire de Matériaux et Structures de Génie Civil, Boîte Postale Orly Sud No. 155, F-94396 Orly Aerogare CEDEX, France
(Received 23 April 1990)

Glass-sphere avalanches have been studied experimentally using a drum partly filled with beads and rotating slowly (Ω) around its horizontal axis. The statistics of the avalanche characteristics (i.e., duration D and size $\delta\Theta$) have been determined as a function of the rotation speed Ω, the sphere diameter d, and the drum length l. The widths of these statistics are broad, but avalanches do not exhibit either periodicity or $1/f$ noise. We conclude also that avalanches are governed by inertia and gravity. We recall then classical results of soil mechanics; we will see that triaxial test results, together with the so-called "critical state" of granular material and the Granta gravel model of sandpiles will make evident and quantify the well-known effects of friction, caging, and dilatancy in granular samples. Using these established results, especially those on the "critical" state of soil, we will demonstrate that the maximum angle of repose of a pile may exceed the angle of friction for initially dense enough materials, but that this leads to a catastrophic event (avalanche). This critical-state approach also allows us to relate the mean angle per avalanche to the mean avalanche duration, using an inertial process, and to predict the avalanche duration. According to our model, the avalanche size is controlled by the difference between the real pile specific volume v and that of the "critical" state v_c; macroscopic avalanches are obtained for $v < v_c$ (i.e., a first-order process), but we expect critical fluctuations (and probably $1/f$ noise) when $v = v_c$ (i.e., a second-order transition). This theory makes a link between the theory of self-organized criticality of sandpile avalanches and experimental data; it links also the Coulomb approach of the stability of a free surface and the dilatancy effect discovered by Reynolds.

I. INTRODUCTION

It is well known that an inclined free surface of a sandpile is still stable as far as its angle to the horizontal plane is smaller than an angle Θ_M; Θ_M is called the maximum angle of repose.[1] These different inclinations are allowed by the existence of different settlements of the balance between gravity and intergranular forces (contact, cohesion, friction, etc.). The precise value of Θ_M seems to depend on packing, grain geometry, and boundary conditions.[1]

As early as 1773, Coulomb[2] introduced a mean macroscopic friction coefficient M to explain these different inclinations of the free surface and has found that Θ_M and M should be related ($M = \tan\theta_M$ for noncohesive granular materials). However, this simple model neither explains the sensitivity of Θ_M to the method of building the pile,[1] nor predicts the existence of an avalanche process instead of a continuous sliding-down flow, when one tilts the pile slowly and tries to slightly exceed Θ_M: it is only at fast rotation speeds Ω that a continuous flow of beads is observed experimentally; but, indeed, at low enough Ω, one observes an intermittent flow,[3-5] which consists of a series of avalanches that readjust Θ below Θ_M followed by stoppages.

Then, Reynolds,[6] in 1885, discovered the concept of dilatancy and its importance in granular motion processes: due to a static interlocking of the grains, a noncohesive granular material cannot flow or change shape without dilating first. The effect of dilatancy on dissipation processes was investigated by Bagnold[7,8] in 1954 and 1966. A large part of these papers is devoted to evaluating the loss due to grain collisions as a function of the shear flow, packing density, and inelasticity of the collisions; however, some of Bagnold's work, in Ref. 8, is devoted to the intermittent motion of a bulldozed pile of noncohesive granular material[8] and is based on a quasistatic analysis. For example, Bagnold attributed the excess of friction, which is generally observed in statics instead of dynamics studies to a microscopic dilatancy effect so, using experimental measures of the difference between friction angles in statics and dynamics, he predicted a periodic motion of the bulldozer.[8]

On the other hand, Bak, Tang, and Wiesenfeld[9-11] (BTW) have recently introduced the concept of self-organized criticality to understand the so-called $1/f$ noise problem. These authors have based their approach on a model (the BTW model) which should also describe the intermittent flow of sand at the free surface of a sandpile inclined at Θ_M, since one way of stating the model is as follows:[9-11] one considers a pile of noncohesive monodisperse spheres laying on a half horizontal plane and an amount of independent similar spheres that are added to the pile on its free surface, one at a time and at random. Let us now assume that the difference of height between two adjacent spheres at the free surface cannot be larger than a given quantity h_0 (this is equivalent to defining a maximum angle of repose Θ_M); it may then occur that the difference of height between a sphere that has just

been added and its neighbors exceeds h_0 so that the local surface is no longer stable; when this occurs, the system tends to restore its equilibrium through a local downhill flow on the free surface, which is governed by a set of simple local rearrangement rules and local flow rules (we will not specify the rules here, since different sets may be chosen and have been investigated[9–14]). One is then interested in the properties of the "quasistationary" state that is reached after adding a tremendously large number of spheres; in particular, one is interested in knowing the size distribution of the flow observed at the free surface in response to adding one grain in a given location; or, one is interested in knowing the amount of beads that fall below the horizontal half plane when a bead is added somewhere on the pile.

So, these authors have computed the statistics of bead avalanches and have found a tremendously broad distribution of avalanche sizes (i.e., the tail decreases as a power law and not exponentially as one would have thought). This result means that the size of the local surface that has to be geometrically reorganized in order to obtain a new equilibrium depends strongly on the dropping location. It was then demonstrated that the BTW model creates spontaneously self-organized critical states leading to properties similar to those in second-order phase transitions and characterized by scaling laws and critical exponents.[9–11] The universality classes of the BTW model have been investigated by Kadanoff *et al.*[12]

From an experimental point of view,[3–5] one observes some fluctuations of the avalanche size around a mean value: the width of the experimental size distribution ranging from about half the value of the mean value. The distribution of sizes is too broad to be considered periodic, as in Bagnold's model of bulldozing[8] (since this model does not predict any size fluctuation), but it is still not broad enough to reflect a $1/f$ noise, as in the BTW model.[9–14] So, one is faced with two alternative theoretical solutions that contradict each other and that do not describe in its full completion the reality.

More recently, Jaëger and co-workers[13] followed an approach similar to the grain inertia regime[7] of Bagnold's calculation for the "grain inertia regime;" they found that the losses of granular material submitted to shear flow depend strongly on the shear rate, so that there exists a minimum of losses at a nonzero finite shear-speed rate. They attribute the intermittency observed in avalanche flow to the existence of this minimum and skip completely a possible discontinuity of the friction coefficient between statics and dynamics, as it has been assumed by Bagnold in his specific model for bulldozing motion.[8] Furthermore, this approach does not explain the fluctuations of avalanche size.

On the other hand, more precisely, soil-mechanics specialists are commonly using a triaxial testing method[16–20] to characterize their granular samples; they have classified and interpreted the main features of the different possible behaviors of a soil as functions of the initial density of this soil, which also governs its dilatancy; furthermore, these tests show that a dilatancy effect is sufficient to bring cohesion between grains from a mathematical point of view, so that the denser the initial packing is, the more cohesive the grains seem to be, the larger the pseudostatic friction is, and the larger the maximum angle of repose will be. However, these tests also show that when dilatancy has occurred, the grains no longer look cohesive so that the dynamic friction angle reaches a limit value smaller than the static one.

So, faced with the intricacy of the problem due to the numerous different theoretical approaches, we have decided to pursue our experimental study of avalanches,[3,4] in order to determine the real basic concepts which govern these phenomena. This paper is then devoted to investigating, both experimentally and theoretically, the properties of bead avalanches. The paper is structured as follows. Section II is devoted to describing the experimental techniques and the different experimental parameters; for instance, we have determined the statistics of the avalanche duration and of their intermittency as a function of the bead diameter, of the rotation speed Ω, and of the number of transverse bead layers. (This last point is important in the BTW model since it determines whether the transverse horizontal direction influences the statistics and the dynamics or not; it is then a measure of the space dimension).

Section III is concerned with experimental data and their main interpretation; for instance, we will discuss whether or not successive avalanches are size correlated, what the influence of a regular lattice is, and how the avalanche size scales as function of the pile size. We will also show that the dynamics of the avalanche studied here is controlled by inertia. At last, we will discuss different finite size effects and the existence of a bistability between the avalanche regime and the continuous-flow regime at large rotation speeds.

In the following sections, we will compare our results to other classical results in soil mechanics that exhibit dilatancy; this creates the nonlinear process that explains the avalanche process.

A major result of triaxial test studies is that any homogeneous sample that remains homogeneous during yielding eventually reaches a constant density ρ_c and a constant friction coefficient M, independent of its initial density. This limit state is called the "critical" state by soil-mechanics specialists[16–19] (in phase-transition terms, this state is obviously not a critical state and we will call it "critical" in order to keep the same notation used in soil mechanics). These results enabled Schofield and Wroth[17] to build their so-called Granta gravel model to describe yielding and its evolution in noncohesive granular material; they have assumed that (i) losses are due to solid friction and are governed by a unique friction coefficient M, (ii) strain is due to a plastic yielding only (no elastic strain), and (iii) the "critical" state exists and is isotropic (this last assumption, isotropy, is not valid in real cases,[20] but we will still consider it valid for the sake of simplicity). We will summarize the theory of Schofield and Wroth[17] in the last part of Sec. IV. Since this theoretical approach requires soil mechanics notation and concepts, Sec. IV appear slightly intricate.

This is why we will derive in Sec. V a simpler theory based on the same approach as the Granta gravel model, but which pertains specifically to the problem of an in-

clined free surface; this will enable us to predict many of the experimental observations and to build a bridge between the different approaches of avalanches. In the following we will discuss some conclusions.

(i) If the pile is denser than the density of its "critical" state, ρ_c, it must dilate before flow occurs; this brings intermittency with large avalanches. In this regime, no $1/f$ noise is observed. The system is similar to Bagnold's model for bulldozing, except that the density of the pile at rest varies after each avalanche. However, the process that creates these spontaneous fluctuations is not yet well identified. As the density controls the difference between the pseudostatic friction coefficient and the dynamic one (i.e., the critical one), it also controls the difference between the largest slope Θ_M of the free surface of a pile at rest and the critical friction angle Φ. According to this, the size of the avalanche depends linearly on $\Theta_M - \Phi$, so that it scales as the pile size for a given initial density. We also think that the difference between the pseudostatic and dynamic friction controls the avalanche dynamics.

(ii) However, if one can control the pile density and keep it at its critical density ρ_c, this theory predicts the absence of the dilatancy effect. In this case, the pile behaves as a true noncohesive Coulomb material governed by the friction angle alone. This system becomes similar to the BTW model, since it is only controlled by the friction coefficient; we expect then that the spontaneous flow at its free surface exhibits $1/f$ noise when the rotation of the free surface is slow enough (i.e., in a case similar to the BTW model).

Due to these remarks on scaling properties of avalanche sizes, we will argue that avalanches at a pile's free surface look like a first-order transition when the pile density is larger than the critical density ρ_c (using the meaning of soil-mechanics specialists), since their size is proportional to the pile size. However when the pile density approaches the critical density of soil, one may observe large size fluctuations, as observed when a system approaches a second-order phase transition. This will allow us to draw a parallel between an avalanche problem and the liquid-gas boiling transition: boiling is a first-order phase transition if the boiling temperature T is different from the critical temperature T_c, but boiling is a second-order phase transition at T_c and exhibits critical fluctuations. So, we think that avalanches exhibit $1/f$ noise and self-organized critical behavior when the pile density is controlled and approaches the critical state density.

II. EXPERIMENTAL TECHNIQUES

A. Principle of the experiment

The principle of the experiment is sketched in Fig. 1: a hollow Duralumin cylinder of radius $R_{\text{cyl}}=9.5$ cm and of length l rotates slowly around its horizontal axis at a constant speed Ω; the rotation is driven by a dc motor, the speed of which is controlled by a microcomputer; the cylinder is partly filled with "monodisperse" glass spheres characterized by a mean diameter d and a distribution width δd of d ($\delta d/d \approx 0.2$).

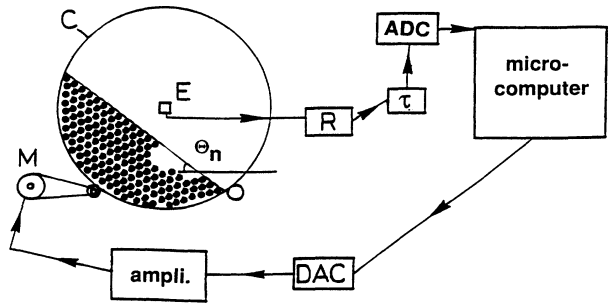

FIG. 1. Experimental setup: E, electret microphone; M, dc motor; R, rectifying diode and lock-in amplifier; C, drum; τ, time constant.

When the rotation speed Ω is slow enough, the angle Θ of repose of the pile's free surface increases continuously until an avalanche occurs, which readjusts Θ below Θ_M. On the contrary, at fast Ω, one gets a continuous flow of glass spheres rolling down on the free surface. We have used the sound emitted by the beads during collisions to detect the bead flow: an electret microphone located in the middle of the drum detects any sound; the signal is then rectified and demodulated by a lock-in amplifier at a frequency corresponding to an eigenmode of the cavity; this increases the signal-to-noise ratio; the rectified and demodulated signal $S(t)$ is then digitized, stored, and analyzed in a microcomputer. An example of $S(t)$ is given in Fig. 2; it has been obtained in the avalanche regime and is made up of a series of peaks, each corresponding to an avalanche.

When the mean time between two consecutive avalanches is much larger than the avalanche duration, one may neglect the drum rotation during avalanches and get the average flux $\langle F \rangle$ of spheres given by

$$\langle F \rangle = (\alpha - \cos\alpha \sin\alpha) l R_{\text{cyl}}^2 \Omega \ , \tag{1}$$

where Ω is the speed of rotation of the hollow cylinder of length l and radius R_{cyl} and 2α is the angle of the drum arch on which the grains lie. $\langle F \rangle$ depends on the filling ratio of the drum through α ($\alpha=\pi$ for half-filled

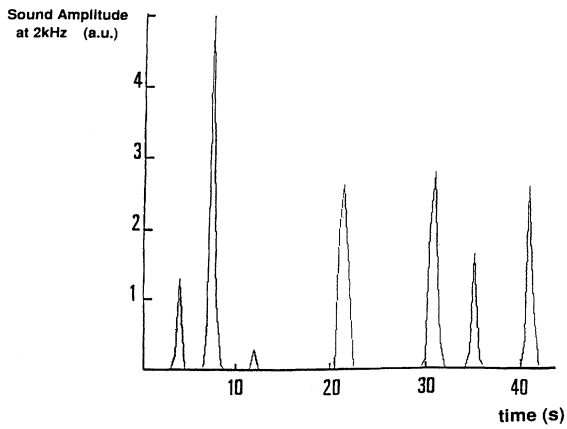

FIG. 2. Typical sound amplitude $S(t)$ as a function of time t; each peak corresponds to an avalanche of spheres.

cylinders). Thus Eq. (1) is also valid in the case of a continuous flow provided that one neglects the thickness of the bead layer at the free surface, which constitutes the continuous flow.

B. Sets of parameters

The different parameters that control the experiment are the inner drum radius R_{cyl}, the drum horizontal length l, the rotation speed Ω, the sphere diameter d, and the angle 2α, which characterizes the rate of filling of the drum. We should also include air humidity, packing density, and electrostatic charges, but they have not been measured nor really controlled. We hope and think that cohesion forces are negligible in our experiment.

The ranges over which we have studied the influence of each parameter are $\alpha \approx 1$, $R_{cyl}=9.5$ cm, $2\text{ mm} \leq l \leq 32$ mm, $0.1°/\text{s} \leq \Omega \leq 10°/\text{s}$, $1\text{ mm} \leq d \leq 10$ mm.

We shall mention that electret-microphone detection does not allow us to study avalanches of spheres with diameters smaller than 1 mm. The larger the beads, the louder the sound emitted during collisions, and the larger the signal-to-noise ratio. However, our results are similar to the data published by Jaëger, Liu, and Nagel,[5] so we may use these data and increase the investigated bead diameter range to 0.5–10 mm or even 0.07–10 mm.

C. Method for analyzing the results

The first method for studying the statistics of avalanches is to compute the autocorrelation function $C(\tau)$ of the signal $S(t)$ through

$$C(\tau)=\int S(t)S(t+\tau)dt \ . \tag{2}$$

A typical result is reported in Fig. 3, which has been obtained with a recording time of 1000 s. The signal which seems noisy, may be interpreted as follows.

Consider first avalanches that are equally spaced and of equal amplitude $S(t)$ is then a perfectly regular comb made up of a series of teeth; the width of any $S(t)$ tooth is the avalanche duration D, and the periodic distance T_1 between two consecutive peaks is the time separating two consecutive avalanches. Thus $C(\tau)$ is a perfect comb; the width of its teeth is proportional to the avalanche duration and the periodic time separating two $C(\tau)$ teeth is the time T_1.

Consider second a series of avalanches that appear quasiperiodically with a mean period T_1 and a small jitter δT_1 around this mean value. In this case, $C(\tau)$ will look like a perfect comb at short times ($\tau < \tau_c = T_1^2/\delta T_1$), but the teeth decrease in amplitude and broaden within time τ_c, so that $C(\tau)$ reaches a constant value equal to D/T_1 at long times.

According to this, Fig. 3 implies that δT_1 is approximately equal to T_1 and that D is approximately one-fourth of T_1. We interpret the long-time fluctuations of $C(\tau)$, which are large, as induced by the small number of avalanches which are stored in the computer (approximately 100). This method then leads to a rather large uncertainty.

However, this interpretation is oversimplified since it does not take into account the large fluctuations of the sound amplitude exhibited by Fig. 2. On the other hand, it would be difficult to take these fluctuations into account since we have no theory that precisely relates the sound amplitude $S(t)$ at time t to the flow of beads rolling down at the free surface.

So, one way to improve the accuracy of our experiment is to increase the number of stored events. This can be done within the same computer memory size if one neglects to treat the whole time dependence of the sound amplitude and keeps in the memory only the times $T_B(i)$ and $T_E(i)$ at which each avalanche begins and ends (i means the ith avalanche). Thus, one may compute the statistics of the avalanche duration D, $D(i)=T_E(i)-T_B(i)$, and of the time $T_1(i)$ separating two successive avalanches, $T_1(i)=T_{B(\text{or }E)}(i+1)-T_{B(\text{or }E)}(i)$. In order to do so, one has to define a threshold S_0 of sound amplitude: if $S(t)<S_0$, there is no avalanche at time t; if $S(t)>S_0$, an avalanche is occurring. For instance, we report in Figs. 4 and 5 the preceding two statistics, respectively. They have been obtained in a 4-mm-length drum with 2-mm-diam spheres and a rotation speed $\Omega = 1°30'/\text{s}$, after storing 1500 avalanches.

As shown in Fig. 4, the statistics of D exhibit two peaks, one ($D_M \approx 2$ s) much larger than the other

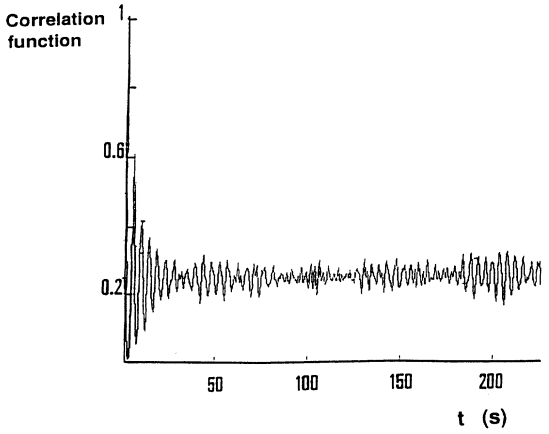

FIG. 3. Time autocorrelation function of the signal $S(t)$.

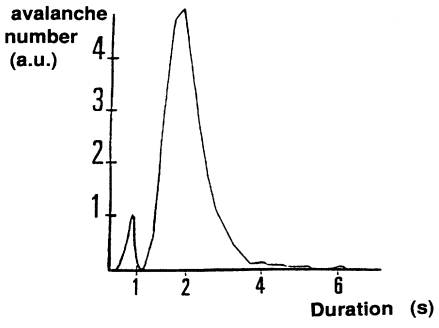

FIG. 4. Typical statistics of the avalanche duration D.

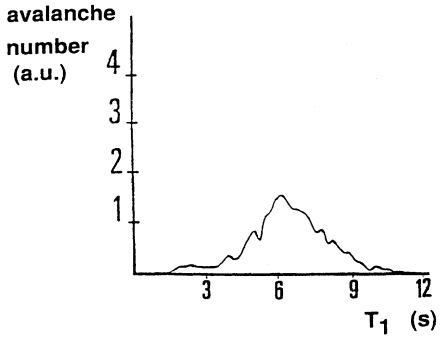

FIG. 5. Typical statistics of the delay T_1 between two consecutive avalanches.

($D \approx 0.8$ s); we have observed that the amplitude of the shorter peak decreases steadily when increasing either the threshold S_0 or the time constant of the lock-in amplifier (cf. Fig. 1). Therefore we interpret this first peak as a problem of noise: small peaks of sound are counted as individual avalanches of short duration located near a large avalanche instead of being included in these large avalanches. This has been confirmed by observing the flow: no small avalanche could be observed. But because of this noise effect, the spheres we wish to study have to be larger than 1 mm in diameter. In the same way, we have checked that as long as the signal-to-noise ratio of $S(t)$ is large, the T_1 statistics depend neither on the S_0 value nor on the way of computing T_1 [i.e., neither using the ending times $T_E(i)$ nor using the beginning times $T_B(i)$].

So, Fig. 4 leads to a mean avalanche duration of about 2 s and a distribution width of 1 s. Figure 5 leads to a mean intermittency time $\langle T_1 \rangle \approx 6.4$ s and to a width $\delta T_1 \approx 3.5$ s. These results seem to disagree with the model of Bagnold[8] concerning the bulldozer motion, since the motion is not periodic, but they disagree also with the BTW model,[9–14] since this model predicts a long tail for the distribution of avalanche size, which is not observed here. Nevertheless, experimental results similar to ours have also been obtained by others for different sizes of beads (i.e., Jaëger, Liu, and Nagel[5]). This improves the validity of our results and demonstrates that such values of the $\delta T_1 / T_1$ ratio are very common.

Thus, Figs. 4 and 5 demonstrate that different avalanche sizes may occur. One may then ask if there is any size correlation between two consecutive avalanches. One way to proceed is to determine the statistics of the time T_N separating $N+1$ consecutive avalanches. The mean value $\langle T_N \rangle$ of T_N is always $N\langle T_1 \rangle$ and does not depend on correlation, but this is no longer true for the width δT_N of the distribution: if avalanches are independent events, one has

$$\delta T_N^2 = N \, \delta T_1^2 \ . \tag{3a}$$

However, if there are series of large avalanches and then series of small avalanches, one has

$$\delta T_N^2 > N \, \delta T_1^2 \ . \tag{3b}$$

If a large avalanche is more likely to occur after a small one and a small one after a large one so that we have two intertwined periodic combs of avalanches, the first one made up of large avalanches and the second one of small avalanches, one gets

$$\delta T_N^2 < N \, \delta T_1^2 \ . \tag{3c}$$

So, by measuring δT_N as a function of N one may determine if size correlations do exist between consecutive avalanches or not.

III. EXPERIMENTAL DATA AND THEIR ANALYSIS

We report exclusively in this section the experimental results obtained with the second method. So, the experiments have been consisting of storing in the computer memory the beginning and ending times of a series of 1500 successive avalanches for each set of parameters (Ω, l, d); the parameter range was given in Sec. II B.

A. No evidence for size correlation between two avalanches running

We have investigated the correlations between successive avalanches using the method described in Sec. II. We report in Fig. 6 a typical example of the variations of δT_N as a function of N for $N = 1, 2, 4, 8, 16, 32$. In the limit of the experimental uncertainty, no size correlation has been found. However, a precise analysis of the width recession for $N = 1$ and 2 is difficult due to the existence of the first peak in Fig. 4.

One can perhaps understand the lack of correlation using Fig. 7, which displays the successive volumes involved in successive avalanches. As spheres flow down from the top to the bottom of the pile, the beginning of the avalanches occurs more likely on the top part of the pile and the avalanches end on the bottom part of it, since the beads are partly stopped by the drum wall. This process implies that the beads do not have enough energy to modify strongly the structure of the underlayer on which top beads were reposing. So, the next avalanche will more likely start on a part of the pile, the structure of

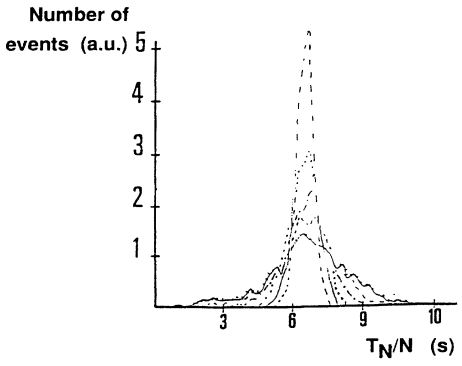

FIG. 6. Typical statistics of the time T_N separating $N+1$ avalanches running in the reduced time unit T_N/N. The regression of the width as a function of N follows Eq. (3a) within the experimental uncertainty, which indicates uncorrelated events.

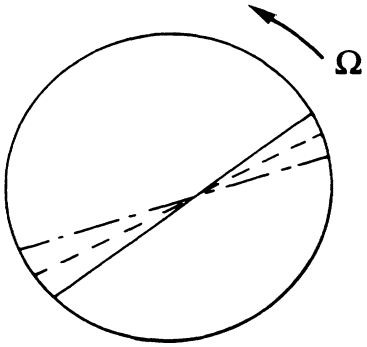

FIG. 7. The geometry of the pile at the ith avalanche (——), at the $(i+1)$th avalanche (— — —), and at the $(i+2)$th avalanche (—·—·—·).

which has not been modified by the previous avalanche; the process that initiates this next avalanche depends on the structure of the top of the pile, which has not been built during the previous avalanche but during a whole set of avalanches, especially those that occurred earlier at time $t=2\alpha/\Omega$. This means that the 60 previous avalanches are important for the pile structure (according to $2\alpha\approx 150°$ and using a mean angle of rotation per avalanche of about 2.5°, as will be determined later).

Another process that amplifies this lack of correlation, which is probably the most important process, is related to the dilatancy property of noncohesive granular material. As we have already mentioned in the Introduction and as we will see in more detail in Secs. IV and V, a pile must dilate first before yielding occurs, so that the denser the pile, the stronger at yield it will be. This is the basis of a nonlinear behavior: assume that the pile begins dilating in a nonuniform manner, then it will become looser in some location and yielding will begin there. This nonlinear effect is responsible for the phenomon commonly observed by soil-mechanics specialists called localization of yieldings, one observes often a condensation of yieldings on surfaces and a creation of localized surfaces of yielding.[21–24]

This localization process contributes to understanding the lack of correlation in the avalanche case. It is only the structure of the top layer that actually moves which is modified and not the underlayer, so that the structure of the uppermost underlayer of the pile is more or less preserved by the avalanche.

B. Statistics of avalanche duration: evidence for an inertial mechanism

We have investigated the dependences of the avalanche duration D as functions of the rotation speed Ω, of the drum length l, and of the sphere diameter d by drawing the probability law of the avalanche duration D for each set of parameters (Ω,l,d). We will consider in this section the results obtained in the small-Q range only, i.e., far away from the transition to the continuous-flow regime; Sec. III E will be devoted to discussion of this last problem.

A typical distribution of avalanche durations is given in Fig. 4, the characteristics of which have been discussed in Sec. II C. Owing to this we have characterized the curves by the duration D_M of the more probable avalanche (i.e., the duration corresponding to the maximum of the second largest peak) and by the width w of this second peak.

We report in Fig. 8 the values of D_M, averaged over different Ω, for different drum lengths l and as functions of the sphere diameter d. Obviously, Fig. 8 exhibits large fluctuations which we do not understand, since the large number (1500) of avalanches taken into account in each datum should give better precision. These fluctuations are likely induced by the uncontrolled variations of a hidden parameter, such as the air humidity, or they may only be due to long-range correlations, the existence of which has been already discussed.

Nevertheless, we can conclude from Fig. 8 that D is more or less independent of d and l and that the mean value $\langle D_M \rangle$ of D_M is 1.4 s. We have also computed for each set of parameters the ratio of w/D_M and have found that its value is independent of the set (d,Ω,l), within the experimental uncertainty:

$$w/\langle D_M \rangle \approx 0.8 \ . \tag{4}$$

Moreover, the data published by Jaëger, Liu, and Nagel,[5] which concern other sphere sizes ($d=0.07$ and 0.5 mm), agree with Eq. (4) and with the $\langle D_M \rangle$ value; this extends the validity range of these behaviors. This is surprising since each avalanche is composed of a few tens or hundreds of spheres in most of our experimental cases, but with more than a few thousands in the case of Jaëger, Liu, and Nagel case. These experimental observations hold in the "microscopic" limit as well as in the "mesoscopic" one.

One may now try to write the mean duration $\langle D_M \rangle$ as a function $f(R_{\rm cyl},d,l,g,\Omega)$ of the different parameters (g is the gravity). The use of dimension analysis leads to the equation

$$\langle D \rangle = A\,(R_{\rm cyl}/g)^{1/2} \quad (\Omega \to 0) \tag{5}$$

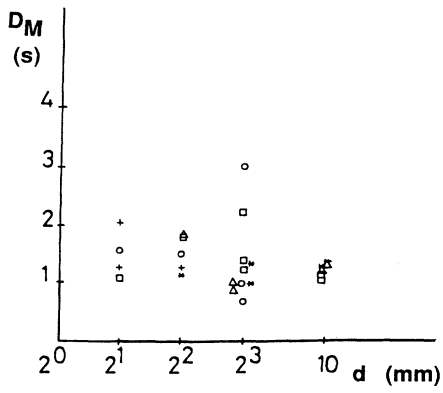

FIG. 8. Small-Ω regime. Duration D_M of the most probable avalanche as a function of the sphere diameter d and for different drum lengths l. (+, $l=2$ mm; △, $l=4$ mm; ○, $l=8$ mm; □, $l=16$ mm; *, $l=32$ mm.)

where A is a nondimensional constant; A is approximately 17. Clearly, Eq. (5) indicates an inertial regime. In Sec. IV and V, we will develop a theoretical argument that supports this result and give an approximate expression for A, based on the existence of a mean angle per avalanche.

C. Statistics of the intermittency between two avalanches: Evidence for a mean angle per avalanche in the inertial regime

In this section, we will still be exclusively concerned with the small-Ω regime. For each set (d,l,Ω) of parameters, we have written the statistics of the time T_1 separating two consecutive avalanches (a typical result of which is given in Fig. 5), and have computed the width-to-mean-value ratios $\delta T_1/\langle T_1\rangle$; we have found it to be independent of the (Ω,l,d) set:

$$\delta T_1/\langle T_1\rangle \approx 0.4 \ . \tag{6}$$

Furthermore (in the $\Omega\rightarrow 0$ regime), the T_1 statistics are always similar to those reported in Fig. 5 so that they never exhibit any long tail in both wings. This clearly means that one can speak of a typical avalanche size $\langle V_{\rm aval}\rangle$ and of a typical size fluctuation $\delta V_{\rm aval}$:

$$\langle V_{\rm aval}\rangle = (\alpha-\sin\alpha\cos\alpha)R_{\rm cyl}^2\Omega\langle T_1\rangle \ , \tag{7a}$$

$$\delta V_{\rm aval} = (\alpha-\sin\alpha\cos\alpha)R_{\rm cyl}^2\Omega\delta T_1 \ . \tag{7b}$$

Combining Eqs. (6) and (7) leads to $\delta V_{\rm aval}/\langle V_{\rm aval}\rangle \approx 0.4$. We have not determined higher-order momenta of Fig. 5, due to the lack of experimental precision; but it is obvious that the third-order momentum is small, since the curve is quasisymmetric around its mean value. So, we may conclude that our results exhibit neither a $1/f$ noise distribution nor a perfect periodicity. These results are then compatible neither with the self-organized criticality approach (no $1/f$ noise), nor with the theory of Bagnold (no perfect periodicity).

We have also measured the mean time $\langle T_1\rangle$ separating two consecutive avalanches for different Ω and found that it varies as $1/\Omega$ (in the $\Omega\rightarrow 0$ regime). This means that we can speak of a mean angle $\langle\delta\Theta\rangle$ of the drum rotation between two successive avalanches.

We have studied the variations of $\langle\delta\Theta\rangle$ as a function of l and d and have found that it may be written as

$$\langle\delta\Theta\rangle \approx 2.5^\circ + G(x) \quad (\Omega\rightarrow 0) \tag{8a}$$

with

$$x = l/d \ , \tag{8b}$$

where $G(x=l/d)$ is a function and is sketched in Fig. 9(c). As a matter of fact, one way of determining and visualizing this relationship is to plot the different experimental values of $\langle\delta\Theta\rangle$ as a function of different abscissas u_i, as we have done in Fig. 9. One expects the points to be dispersed at random in the $(\langle\delta\Theta\rangle,u_i)$ plane if there is no relationship between $\langle\delta\Theta\rangle$ and u_i; but one expects the points to be aligned on some curve exhibiting noise, for an appropriate value of u_i.

So, according to Fig. 9, the appropriate parameter is $x=l/d$, and according to Fig. 9(c), $G(x)$ is always positive and tends quickly to 0 as soon as x is larger than $x_c=4$; $G(x)$ may be as large as 7° for small values of x ($x=1$). The physical meaning of the variations of $G(x)$ will be discussed in Sec. III D.

What we want to emphasize here is that the asymptotic value of $\langle\delta\Theta\rangle$ at large x is 2.5°; this is also the value obtained by Jaëger, Liu, and Nagel[5] for slightly smaller glass spheres (diameter of 0.54 mm). So, for drums much thicker than one bead in diameter (i.e., $x\gg x_c$), $\langle\delta\Theta\rangle$ is independent of l and Ω, and $\langle\delta\Theta\rangle$ may actually be considered as the true mean angle per avalanche: in particular, this means that the number $N_{\rm aval}$ of beads per avalanche increases linearly with increasing l and decreases as $(1/d)^3$ when increasing the bead diameter d (within the limit of our experimental precision).

D. Influence of packing in the avalanche characteristics: 2D order→3D disorder crossover

As we have already mentioned in the preceding paragraphs, we have found experimentally that $\Omega\langle T_1\rangle$ is a constant so that we may speak of a mean angle per avalanche $\langle\delta\Theta\rangle=\Omega\langle T_1\rangle$; we have also found that $\langle\delta\Theta\rangle$ data obey Eq. (8), which means that they depend only on the ratio $(x=l/d)$ of the cylinder length l to the sphere diameter d. x is then the number of transverse vertical layers of beads that are contained by the drum. We have determined that $\langle\delta\Theta\rangle$ reaches an asymptotic value (2.5°) as soon as $x=l/d$ is larger than a characteristic value $x_c=4$. So, as soon as the length of the drum contains more than four vertical layers of beads parallel to the vertical surfaces of the drum, the avalanches reach their 3D characteristics.

Let us now discuss the physical meaning of $G(x)$ and try to prove that $G(x)$ reflects the change of the packing characteristics between a two-dimensional sample and a three-dimensional one.[25]

Let us first remark that trying to build a dense packing of spheres by only maximizing its density at a local scale leads first to an ensemble of hexagons in 2D space; trying now to get a local dense packing of this ensemble of hexagons leads to an ensemble of larger hexagons and the iteration of this procedure leads eventually to the well-known triangular lattice. Unfortunately, the same iterative procedure of packing generates a disordered structure in a 3D space: the first step leads to an ensemble of tetrahedras and the second one to the packing together of this ensemble of tetrahedras (instead of hexagons), for which it is known that the densest packing cannot completely fill the 3D space[25] and always leads to the existence of voids in a large proportion. This 3D packing procedure creates in general lacunae at random, which explains the existence of a great number of defects in the structure. (However, one can obtain a 3D lattice structure, but this requires a very careful packing procedure or the use of long-range forces as electric forces.)

It is indeed commonly observed that a 2D packing of monodisperse spheres or cylinders exhibits a regular hexagonal lattice structure and that a 3D one is quite disor-

dered. Furthermore, it is also commonly observed that the insertion of a flat surface in a disordered 3D packing reorganizes this random structure into an ordered triangular lattice near the flat surface. Moreover, it has also been measured that such a flat surface no longer influences the 3D disordered structure after a thickness of two or three layers,[25] so that $x_c=4$ may correspond to twice this number of layers.

So, it seems to us that (in the small-Ω limit) the large values of $\langle \delta\Theta \rangle$ observed for small $x=l/d$ values are likely induced by a strong influence of the packing geometry on the avalanche process. Therefore, the variations of $\langle \delta\Theta \rangle$ versus $l/d=x$ at small x reflect an order-to-disorder transition and not a real two-dimensional to three-dimensional crossover behavior. However, these results could also be induced by a change of density or a change of pore connectivity between the 2D and 3D packings.

Nevertheless, we think that the important quantity is the so-called dilatancy,[6,16–18] which is an empirical quantity that varies from material to material and from packing to packing. This is supported by the similarity of behavior we have found between our results and classical results on yieldings of soil, as we will argue and develop in the next sections. For instance, soil-mechanics specialists know how to get a 2D disordered packing of polydisperse cylinders that behaves as a 3D packing of spheres or grains; this is the so-called Schneebeli material.[26] It would be interesting to determine the avalanche characteristics in such a medium and to compare them to our data.

E. Crossover region between the intermittent flow regime and the continuous-flow regime: Bistability and finite-size effects

Our experimental data that concern the avalanche statistics in the fast-Q limit have exhibited in a few cases large fluctuations from one series of experiment to another, as if our results were depending on some hidden and

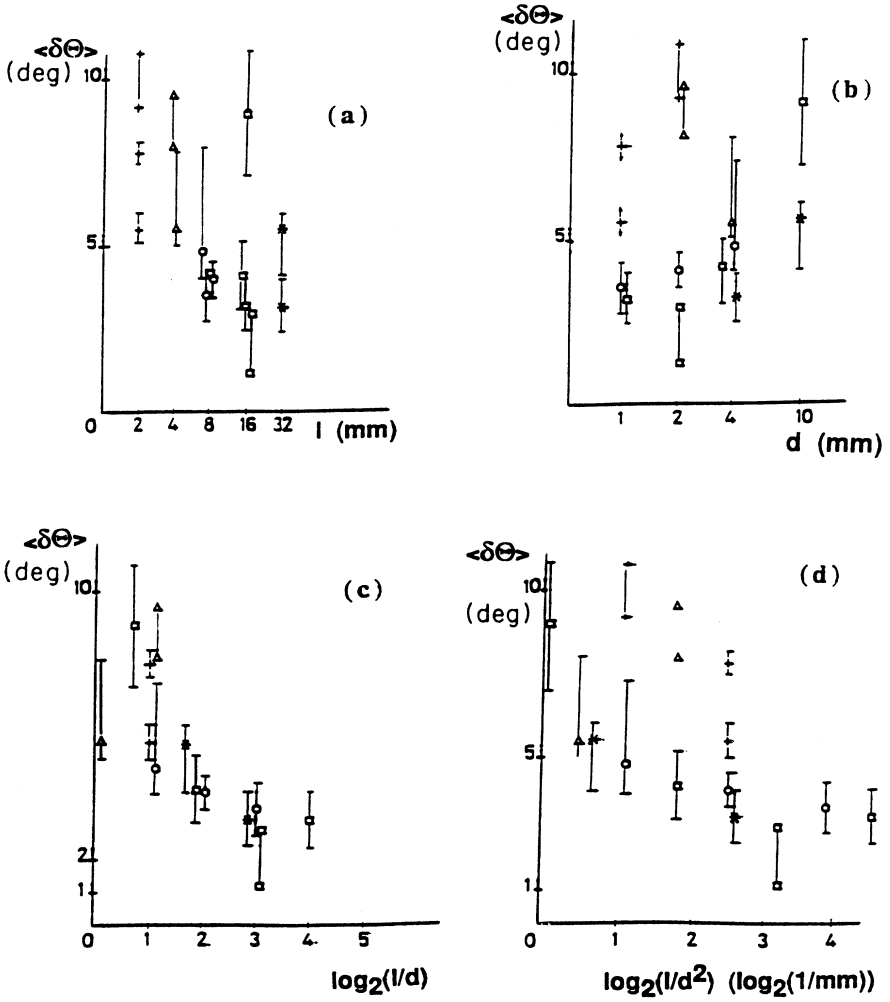

FIG. 9. Small-Ω limit. Plot of the mean angle of rotation $\langle \delta\Theta \rangle$ per avalanche vs (a) the drum length l, vs (b) the sphere diameter d, vs (c) l/d, and vs (d) l/d^2. (+, $l=2$ mm; △, $l=4$ mm; ○, $l=8$ mm; □, $l=16$ mm; *, $l=32$ mm.)

uncontrolled parameter. Therefore it seems to us that much more work is needed to elucidate the different possible behaviors and their range of observation in the large-Ω limit. But now we will try to sketch a few ideas and features.

First, we have always observed that the mean angle per avalanche $\langle \delta\Theta \rangle$ always increased when Ω increased; most of the time, the increase was linear with Ω, until the measure was no longer possible since the system had reached the continuous-flow regime. However, in a few cases that were always concerned with small l/d values ($l/d=1$ or 2), we observed a divergence of this mean angle $\langle \delta\Theta \rangle$ when Ω approached a well-defined Ω_c. When this divergence was observable, the statistics of the avalanche duration D and of the time T_1 separating two running avalanches were quite similar: They contained a large peak at short time followed by a long tail. The characteristics of the peak were approximately the same as the characteristics of the principal peak of Fig. 4. The long tail has an amplitude of about 0.2 times the amplitude of the principal peak and it spreads over a characteristic time that drastically depends on Ω. We explain the similarity of the two statistics (on D and on T_1) by the fact that the flow is more or less continuous with erratic stoppages, so that the real avalanche duration lies very near the time between the beginning of two avalanches.

However, this result seems to us rather surprising since we have also obtained that the avalanche–continuous-flow transition exhibits a bistability that is observed within a precise range of Ω:

$$\Omega_{c1} < \Omega < \Omega_{c2} \tag{9a}$$

with

$$\Omega_{c1} \approx 0.5\Omega_{c2} \tag{9b}$$

and

$$\Omega_{c1} \approx 1.6^\circ/\mathrm{s} \approx \langle \delta\Theta \rangle / D_M \ . \tag{9c}$$

This means that when the rotation speed Ω lies between these two extreme values Ω_{c1} and Ω_{c2}, one may observe either a continuous flow or a series of avalanches, and one may also observe a change of flow regime when hitting the drum. Furthermore, if one starts at $\Omega=0$ and begins increasing Ω slowly and continuously (without hitting the drum), one observes the avalanche regime until Ω reaches Ω_{c2}; this regime then suddenly becomes unstale and a continuous flow is then observed at larger Ω. Similarly, one observes continuous flow until $\Omega=\Omega_{c1}$ when one continuously decreases Ω from a value faster than Ω_{c2}, but below Ω_{c1} one can only observe a series of avalanches.

This hysteresis loop [Eq. (9)] is the signature of a first-order transition.[27] The process which governs it is not yet determined. Nevertheless, this hysteresis loop shall also be observed for any size of spheres as long as no finite-size effect occur; this explains why we have not observed any divergence of the avalanche duration D and of the mean angle $\langle \delta\Theta \rangle$ between two avalanches in most experimental cases. But we may also conclude that the divergences of D and $\langle \delta\Theta \rangle$ obtained in a few cases are likely due to an enhancement of fluctuation effects which reduce the first-order transition to a second-order one. As this reduction to a second-order transition is only observed at small enough l/d ratios, it then reveals either a change between 2D and 3D physics, or it may be simply induced by a finite-size effect. Considering the second hypothesis (finite-size effect) and taking into account the 2.5° per avalanche, the sphere diameter $d=2$ mm, the drum radius $R_{\mathrm{cyl}} \approx 100$ mm, and the drum length $l=4$ mm lead to an avalanche size of 100 spheres. Therefore, 100 beads is the maximum size where finite-size effects may be observed.

We cannot finish this section without quoting two other important works that reveal perhaps some other finite-size effects. The first work concerns the results obtained by Fauve, Douady, and Laroche[28] in much longer cylinders; they found that their series of avalanches become more periodic at large Ω, so that the distribution of T_1 becomes more regular. Furthermore, they observed a transverse propagation of their avalanches along the horizontal direction of the pile's free surface; this obviously means the existence of a transverse horizontal coupling of flows. As these effects have not been observed with our setup, they are likely to reveal another finite-size effect in our experiment.

Recently a $1/f$ noise has been recorded for a flow of sand at a free surface of a finite conic sandpile;[29] this $1/f$ noise disappears when the pile height increases. We think that this $1/f$ noise is due to the occurrence of a quantification effect that is induced by a height h of the pile that is too small compared to the sphere diameter d. We consider a finite conic pile and label Θ the angle of the cone surface to the horizontal plane; this angle Θ cannot be determined with better accuracy than $\delta\Theta_q = d \sin\Theta / h$. Hence, if this $\delta\Theta_q$ becomes larger than the mean variation $\langle \delta\Theta \rangle$ of the surface angle after the avalanche (i.e., $2.5^\circ = \langle \delta\Theta \rangle > \delta\Theta_q$), we may expect that $\langle \delta\Theta \rangle$ no longer has any physical meaning, so that the system behaves in a different manner. We think that the $1/f$ noise reported in Ref. 29 is due to such finite-size effects, and perhaps quantification makes the system obey the BTW model. In our experimental case $h/\sin\Theta \approx 2R_{\mathrm{cyl}}$, so that our experimental $\langle \delta\Theta \rangle$ values have been always larger than $\delta\Theta_q \approx d/(2R_{\mathrm{cyl}})$, even when we have used 10-mm-diam spheres due to the larger values of $\langle \delta\Theta \rangle$ at small l/d ratios.

IV. CLASSICAL TRIAXIAL TEST RESULTS IN SOIL MECHANICS

To interpret these avalanche results in more detail, let us introduce the triaxial testing method of soil mechanics,[16–18] and describe the behavior this method may predict or reveal.

A. Triaxial test method

A triaxial cell allows us to apply to a granular sample three different stresses $(\sigma_1,\sigma_2,\sigma_3)$ in the three different principal directions (x_1,x_2,x_3) perpendicular to one

another. The experiment consists of varying any of these stresses continuously, keeping the others constant, and measuring the three strains $(\varepsilon_1,\varepsilon_2,\varepsilon_3)$ induced along these three principal directions. However, most of the experimental devices use a cylindrical geometry, so if the sample is kept homogeneous all along the test, the axial symmetry is preserved and one has $\sigma_2=\sigma_3$ and $\varepsilon_2=\varepsilon_3$. We will only consider here such an axial setup.

In this case, five parameters are important: p, q, q/p, ε_q, and ε_v. One defines the mean stress as $p=(\sigma_1+2\sigma_3)/3$, which is a quantity similar to the pressure in a liquid; the deviatoric stress $q=\sigma_1-\sigma_3$ is the shearing force; the deviatoric level q/p is the shearing level. In a granular material, we expect that this deviatoric level q/p cannot overpass a given value that is related to the friction coefficient in the classical Coulomb approach. The deviatoric strain $\varepsilon_q=2(\varepsilon_1-\varepsilon_3)/3$ controls more or less the sample contraction or extension along x_1; at last, the volumetric strain $\varepsilon_v=\varepsilon_1+2\varepsilon_3$ measures the change of volume of the sample. A typical setup is sketched in Fig. 10. A plastic bag of cylindrical shape contains the granular material. The top and bottom surfaces of the bag are made up of two rigid plates that act as pistons, so that one may add some weight q on the top piston. This bag is immersed in a container full of liquid, the pressure of which p is controlled and may be varied. ε_v is given by the change of the volume of liquid in the container and ε_1 is obtained by measuring the variation of distance between the two pistons. One may then compute ε_q from the ε_1 and ε_v values $(\varepsilon_q=\varepsilon_1-\varepsilon_v/3)$. We will use the classic sign convention of soil-mechanics specialists: ε_v will be chosen as positive when the system contracts and when liquid flows into the container.

Triaxial extension or compression tests may be carried out by keeping constant either the stress rate $d\sigma_1/dt$ or the strain rate $d\varepsilon_1/dt$. But these rates are kept sufficiently small so that the sample stays in a quasistatic equilibrium at any time. During an experiment, one measures p, q, ε_1, and ε_v as functions of time t. One then plots the deviatoric stress ratio q/p and the volumetric strain ε_v as functions of the deviatoric strain $\varepsilon_q=\varepsilon_1-\varepsilon_v/3$.

B. Typical experimental results obtained with a triaxial cell

We report in Fig. 11 three typical behaviors of granular samples obtained with a triaxial cell. Each behavior is characterized by a set of two curves, i.e., q/p versus ε_q and ε_v versus ε_q; they have been obtained by keeping small and constant the $d\varepsilon_1/dt$ rate. They concern the same material initially packed in three different ways (the solid lines correspond to an initial very dense packing, the dashed lines to an initially very loose material, and the dotted lines to an intermediate density). Furthermore, the grains of this material may be considered perfectly rigid so that we are only testing perfect plastic distorsions.

The q/p versus ε_q variations of Fig. 11 indicate that the deviatoric stress ratio q/p tends toward the same lim-

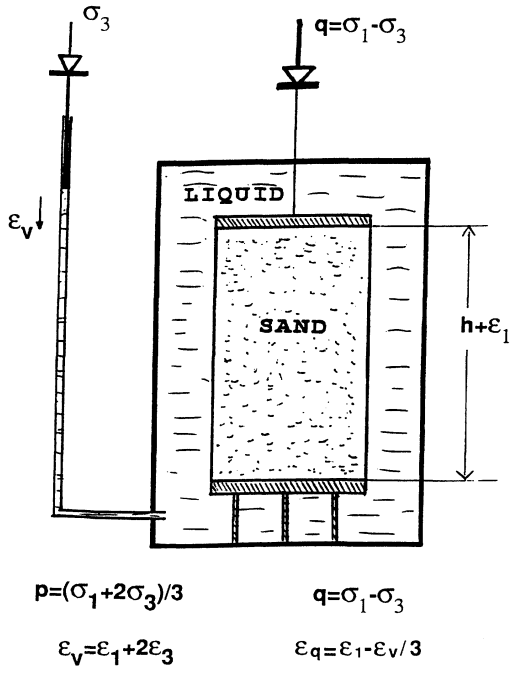

FIG. 10. Sketch of a triaxial cell. A cylindrical plastic bag is closed by two horizontal flat pistons and contains the granular material under investigation. It is immersed in a container full of liquid. One controls the liquid pressure p and the weight q added on the upper piston. One measures then the change ϵ_1 of distance between the two pistons and the amount ϵ_v of liquid which flows from the container as function of q, p, or q/p.

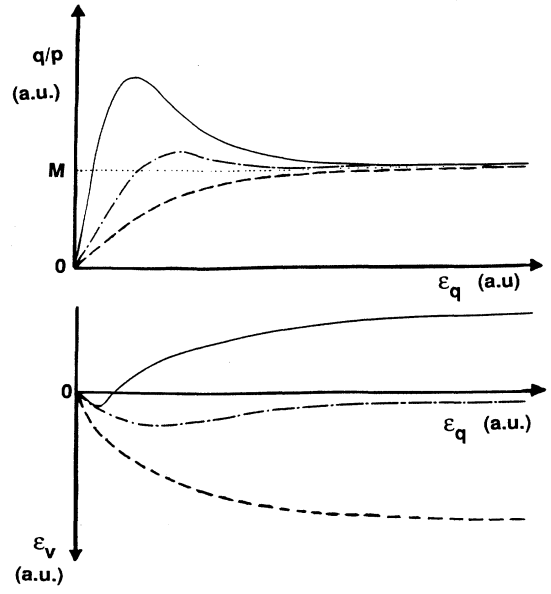

FIG. 11. Three typical behaviors for the same material packed in three different ways, as one finds when one uses a triaxial cell (——, dense packing; — — —, loose packing; —·—·—·, intermediate packing density). p (and q) is the mean (and deviatoric) stress, ϵ_1 is the strain in direction 1, ϵ_v is the volume decrease, and $\epsilon_q=\epsilon_1-\epsilon_v/3$.

it value M at large ε_q strains, independent of the initial density of the packing. Furthermore, a systematic investigation has demonstrated that M is independent of the mean stress p; it depends only on the nature of the material and may then be considered as an intrinsic parameter which corresponds to the macroscopic friction coefficient. Soil-mechanics specialists say that the material is in its "critical" state when the material has yielded and when its q/p value has reached M; it appears also that the density ρ_c of the pile in its critical state depends only on the value of the mean stress p.

However, the way the material reaches the critical state depends on the initial packing density. Figure 11 shows that when the initial sample is very loose, the ratio q/p increases monotonically and the material is always contracting (as one can see from the ε_v versus ε_q variations). On the contrary, for an initial sufficiently dense packing, the deviatoric stress ratio q/p begins increasing, crosses the $q/p=M$ line, then reaches a maximum q_M/p which depends on the initial packing density and then decreases before reaching the M value asymptotically. If one looks at the same time at variations of the volumetric strain ε_v (cf. Fig. 11), one sees that the material is first contracting (ε_v increases within our sign convention), until the q/p ratio crosses the $q/p=M$ horizontal line. It is then dilatant since it reaches an asymptotic value. Looking now at the density ρ_c of the material at this final state (i.e., the so-called soil-mechanics "critical" state[17]), one finds experimentally that it is independent of the initial density, so that the different asymptotic values of ε_v are only reflecting the differences of the volume change between the initial and the "critical" states, which depends only on the initial density.

At this stage of the paper, we want to emphasize two points. First, we have considered a material with rigid grains, such as sand. The elastic strain of this material is then negligible so that most of the strain in Fig. 11 involves plastic irreversible yielding. It might then occur (and it does) that under some special test procedure a finite value of the deviatoric stress ratio q_0/p is required to get a small yielding. Thus, the curves in Fig. 11 may contain a segment of the vertical axis from 0 to the ordinate q_0/p. For instance, this is observed when the test is carried out after a first loading-unloading cycle or when the material is built in a given hardening way.

The second point concerns the instability of a packing which has reached its q_M/p maximum value and has been submitted to a $d\sigma_1/dt=$const triaxial test: a slight increase of q is no longer possible at this maximum of q and a microscopic $d\varepsilon_q$ response is impossible too, so that the packing is unstable and a macroscopic motion, which is often a failure, occurs. This is the rather large difference between triaxial tests carried out under strain- and stress-rate control.

Before we give a theoretical basis for understanding these results let us return briefly to the problem of bead avalanches and to its physical analogy with the triaxial test results. For instance, one is interested in the instability of the inclined free surface of a pile in the avalanche problem. It is obvious that the mean stress p and the deviatoric stress q of a point of the pile both tend toward 0 when the distance of this point to the free surface approaches 0, since these two quantities p and q depend on the weight and height of the matter above the considered point. However, it is also obvious that shearing exists near this free surface so that q/p is different from 0 near the free surface and tends toward a given limit that is controlled by the angle Θ of inclination of the free surface: the larger Θ is, the larger the q/p ratio will be. On the other hand, we have sketched in Fig. 1 a typical setup for the avalanche study. This setup works by controlling the rotation speed $\Omega=d\Theta/dt$ so that it also controls the rate of increase $d(q/p)/dt$ of the deviatoric stress ratio.

So, let us assume that the initial packing is initially dense enough so that q/p may exceed M ($\rho>\rho_c$). According to Fig. 11, only very small yielding will occur as far as q/p as not reached its maximum value q_M/p, but a macroscopic event (the avalanche) will occur just when q/p tries to exceed q_M/p. We then interpret the angle Θ_B at which the avalanche begins as the value at which q/p has just reached its maximum value q_M/p, for a given density; the avalanche that occurs after may only be stopped when q/p reaches a value smaller than M. So the avalanche stops at an angle Θ_E at most equal to Φ, where we have labeled Φ the angle of the free surface which corresponds to $q/p=M$. Φ is Coulomb's angle of friction.

C. The Granta gravel (Ref. 30) model and triaxial cell

In the preceding section, we saw that any granular material submitted to large plastic yielding and kept homogeneous reaches a state where the stress-strain law no longer depends on the initial state. This state has been called the "critical" state of soil, and it is characterized by its specific volume v_c and its internal friction angle Φ. It has been found experimentally that v_c is independent of the initial specific volume v of the soil but depends on the mean stress p at which yielding occurs. Remarkably, Φ has been found to be independent of the initial state, of v_c, and of p, so that it may be considered as an intrinsic parameter playing the part of a perfect internal friction angle in the manner described by Coulomb.

This has led Schofield and Wroth[17] to introduce a simple model to describe drained noncohesive granular materials: their so-called "Granta gravel" model assumes that the medium is made up of rigid grains and that it is either rigid or submitted to a plastic strain (no elastic strain). Furthermore, they have assumed that this Granta gravel reaches a "critical" state at large yieldings which is isotropic and defined by the laws

$$q_c=Mp\ , \tag{10a}$$

$$v_c=\Gamma-\mu\ln p\ , \tag{10b}$$

where M, Γ, and μ are adjustable parameters which depend only on the material nature. In Sec. IV A (cf. Fig. 10), we have defined the deviatoric stress as $q=\sigma_1-\sigma_3$, the mean stress as $p=(\sigma_1+2\sigma_3)/3$, the volumetric strain as $\varepsilon_v=\varepsilon_1+2\varepsilon_3$, and the distortional strain as $\varepsilon_q=2(\varepsilon_1-\varepsilon_3)/3$. $\sigma_1,\sigma_2,\sigma_3$ are the three principal stresses and $\varepsilon_1,\varepsilon_2,\varepsilon_3$ are the three principle strains of the material.

The index c labels the "critical" state; q_c and v_c are then the deviatoric stress and the specific volume of the "critical" state of the Granta gravel model at mean stress p.

Taking into account these assumptions, Schofield and Wroth[17] have calculated the plastic yield curve of Granta gravel as follows. Consider a Granta gravel at a given specific volume v; apply to it a stress so that it stays at the limit of stability (i.e., without exhibiting strain). It is then characterized by the set $(p,q,\varepsilon_v=0,\ \varepsilon_q=0)$. Apply to it now a slight increment of stress $(\delta p,\delta q)$ so that it yields to $(\delta\varepsilon_v,\delta\varepsilon_q)$. The yielding is stable if[17]

$$\delta p\ \delta\varepsilon_v+\delta q\ \delta\varepsilon_q\geq 0\ , \tag{11a}$$

but the total energy that is released is dissipated through friction, so that we have

$$p\ \delta\varepsilon_v+q\ \delta\varepsilon_q=Mp|\delta\varepsilon_q|\ . \tag{11b}$$

We will now focus on what is occurring in a triaxial contraction test, i.e., the case of a length reduction. In such a case one has $\delta\varepsilon_q>0$ for soil-mechanics specialists. At the limit of stability [i.e., Eq. (11a)=0], Eq. (11) leads to

$$\delta p\ \delta\varepsilon_v+\delta q\ \delta\varepsilon_q=0\ , \tag{12a}$$

$$\delta\varepsilon_v=(M-q/p)\delta\varepsilon_q\ . \tag{12b}$$

Therefore, combining the two preceding equations leads to

$$\frac{dq}{dp}=-\left[M-\frac{q}{p}\right]\ . \tag{13}$$

The integration of Eq. (13) leads to the family of yield surfaces (p_Y,q_Y)

$$q_Y/(Mp_Y)+\ln(p_Y)=\text{const}=\ln(p_u)+1\ , \tag{14}$$

where the constant of integration (const) has been rewritten as $\ln(p_u)+1$. A sketch of the yield curve is given in Fig. 12. The maximum value of p is $p_M=ep_u$. q_Y is maximum at $p_Y=p_u$ and its maximum value is Mp_u. This point $(q_Y=Mp_u,\ p_Y=p_u)$ is the critical state $(q_c,\ p=p_u)$, since there is no volume change according to Eq. (12b). We will see later that it is an attractive point, but let us first demonstrate that yielding occurs when the (p,q) trajectory crosses the yield curve from the inner part to the outer part of the plane (i.e., stable configurations are contained between the p axis and the yield curve, which we call the inner part of the plane). In the case of length reduction $(\delta\varepsilon_q>0)$, yielding occurs when Eq. (11a) is strictly positive:

$$\delta p\ \delta\varepsilon_v+\delta q\ \delta\varepsilon_q>0\ . \tag{15}$$

Yielding also obeys the dissipation equation [Eq. (11b)] which implies that $\delta\varepsilon_v=(M-q/p)\delta\varepsilon_q$. Replacing $\delta\varepsilon_v$ by $(M-q/p)\delta\varepsilon_q$ in the inequality (15) and remembering that $\delta\varepsilon_q$ is positive lead to

$$\delta p\,(M-q/p)+\delta q>0\ . \tag{16}$$

Equation (16) shows what we wanted to prove: that yielding occurs when the (p,q) trajectory crosses the yield curve from the inner part to the outer part of the plane, in the case of a length reduction.

We still consider a length reduction and a state on the yielding surface (p_Y,q_Y). According to Eq. (11b), which is the equation that governs dissipation processes, one has

$$\delta\varepsilon_v=(M-q_Y/p_Y)\delta\varepsilon_q\ . \tag{17}$$

As ε_v is positive when the specific volume decreases, Eq. (17) leads to three different variations of the specific volume v of the material depending on the value of p_Y compared to p_u:

(i) v increases when $p_Y<p_u$ and $q_Y>Mp_Y$;

(ii) v does not change when $p_Y=p_u$ and $q_Y=Mp_Y$;

(iii) v decreases when $p_Y>p_u$ and $q_Y<Mp_Y$.

Therefore the point $(p_Y=p_u,\ q_Y=Mp_u)$ is the critical state. Its specific volume is given by Eq. (10b): $v_c=\Gamma-\mu\ln(p_u)$. We will say that case (i) is the case of a material which is strong at yield since it exhibits a pseudofriction coefficient $M'=q_Y/p_Y$ larger than M. This is due to the fact that the material has to dilate when yielding occurs. Case (ii) is the "critical" state case; the system exhibits its real friction coefficient M and it neither dilates nor contracts. Case (iii) corresponds to a material which contracts when it yields. It is said to be weak at yield since it exhibits a pseudofriction coefficient $M'=q_Y/p_Y$ smaller than the real one.

The yield curve that corresponds to Eq. (14) has been obtained for a given material characterized by its specific volume v_1. So, Eq. (14) is the set of points (p_Y,q_Y) which is at the limit of stability for this material. We take this material and apply to it a stress characterized by $p=p_u$ and $q=0$. We then increase q and keep p constant. According to Fig. 12, the material will not yield till $q=Mp_u$, i.e., till it reaches its "critical" state. v_1 is then related to p_u by Eq. (10b). One gets

$$p_u=(\Gamma-v_1)/\mu\ , \tag{18a}$$

$$q_c=Mp_u\ , \tag{18b}$$

and the yield curve is then completely determined by v_1.

Consider now the same material at a new specific volume v_2. Its yield curve will be also expressed by Eq. (14), but with a different constant $p_u'=(\Gamma-v_2)/\mu$. The

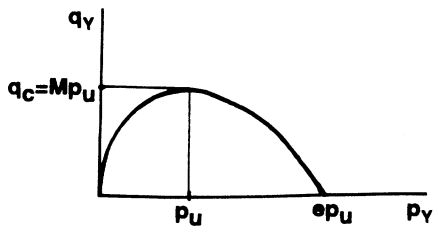

FIG. 12. The yield curve (p_Y,q_Y) of the Granta gravel model, i.e., the set of (p,q) points of the pq plane for which the Granta gravel model becomes unstable. The amplitude p_u is a parameter which depends on the Granta gravel density (the denser it is, the larger p_u is).

two yield curves then have the same shapes; they both start at the origin ($p_Y=0$, $q_Y=0$); their q maxima have the respective coordinates $(p_u, q_c=Mp_u)$ and $(p'_u, q'_c=Mp'_u)$. Their p maxima are, respectively, $(ep_u,0)$ and $(ep'_u,0)$. These two curves do not cross each other and are tangent at the origin. The larger curve delimits a surface with the horizontal axis which contains the other curve. We will call the larger curve the outer curve and the smaller curve the inner curve. They correspond, respectively, to the denser medium and to the looser medium, according to Eq. (18).

One may now consider a whole set of the same material at different specific volumes and conclude that this material is characterized by a whole set of "concentric" yield curves which obey Eq. (14). The larger the yield curve, the denser the material.

Consider a material of a given specific volume v. This defines p_u, according to Eq. (18). Apply to this medium a mean stress p larger than p_u so that the medium is called "weak at yield." Then increase q continuously until yielding occurs. When the material begins yielding, it also contracts itself due to Eq. (17) so that it will become denser and its new yielding curve will be outside the last one. Thus, this means that an increase of q is required to get a new yielding; the medium is stable and the transformation stops when achieved. Consider now the same material which is "strong at yield" ($p<p_u$) and increase q until yielding occurs. In this case, yielding induces dilatancy, according to Eq. (17), so that the material evolves and tries getting a new yield curve which will be inside the preceding one. This means that yielding will still continue as far as q is kept constant and is not reduced quickly. This case eventually leads to a macroscopic event and the only way to prevent such a macroscopic yielding is to control precisely the strain rate.

These results may be summarized in the same manner as the experimental triaxial test results. We report then in Fig. 13 the three typical results Schofield and Wroth[17]

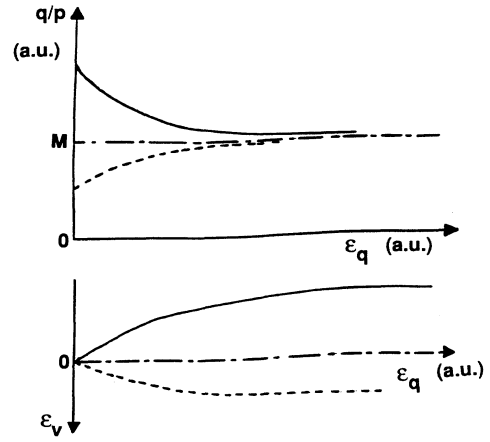

FIG. 13. The three typical behaviors of the Granta gravel model when it is submitted to a triaxial test. ——, dense packing; — — —, loose packing; —·—·—·, the Granta gravel model at critical density. p (and q) is the mean (and deviatoric) stress. ϵ_1 is the strain in direction x_1, ϵ_v is the volume decrease, and $\epsilon_q=\epsilon_1-\epsilon_v/3$.

have predicted by applying their Granta gravel model. We have plotted the q/p ratio as a function of ε_q, and ε_v as a function of ε_q, for a Granta gravel model with three different densities. Indeed, these theoretical curves compare well to experimental data (Fig. 11).

V. RETURN TO AVALANCHES USING GRANTA GRAVEL MODEL

We reported in Sec. IV typical experimental results obtained with a triaxial cell on noncohesive soils and the way soil-mechanics specialists have explained these results. Indeed, their interpretation is not only in complete agreement with the pioneering works of Coulomb[2] and Reynolds,[6] but it links them together within a unified scheme where the effect of dilatancy is taken into account and where losses have been assumed to depend exclusively on solid friction, characterized by a unique friction coefficient characterized by M. The slight differences between the experimental results and the model may be attributed to the existence of stress-induced anisotropy in real systems, the effect of which has been neglected in the model for the sake of simplicity.

However, even as it is (i.e., under the isotropy assumption), the model may look slightly intricate due to the large amount of specific notation which has been introduced in order to keep it general and to describe any kind of yielding. At this stage of the paper, it is worth recalling that a triaxial test looks like a bulldozing problem where the earth is loaded on top. So, even if bulldozing (and triaxial test) is a simple experiment, it remains more intricate than the problem of the stability of an inclined free surface. For instance, Coulomb[2] had already demonstrated that bulldozing exhibits two different inclinations of the sliding plane depending on whether the bulldozer is pushing the earth forwards or if it moves backward pushed by the falling earth. This is why most of our discussion in Sec. IV and most of the equations derived there are only valid in a contraction triaxial test, or in the case of a backward motion of a bulldozer pushed by a pile of earth submitted to a vertical loading. Our theoretical approach of Sec. IV completes the Bagnold approach of the bulldozing problem.[8] It especially quantifies the effect of the pile density on the periodicity of the motion and relates it to the mean stress applied to the pile.

Thus, the problem of the stability of an inclined free surface is conceptually simpler than the bulldozing problem, since there is only one way of sliding. It is then worthwhile to derive a theory simpler than the general one reported in Sec. IV, which describes the avalanche problem.

A. Granta gravel (Ref. 30) model of the stability of an inclined free surface: dilatancy effects in the avalanche process

In this paper, we want to apply the Granta gravel model to the problem of avalanches in a simpler manner than in Sec. IV in order to demonstrate that the avalanche size depends on the difference $(v-v_c)$ between the real specific volume v near the free surface and the specific

volume v_c of the so-called critical state of Granta gravel. However, we will try to keep the notation as similar to that in Sec. IV as possible in order to make the theoretical part of Sec. IV more readable.

The outline of this part is as follows. First of all, we will recall the basic assumptions of the Granta gravel model on which we will base our calculations. We will then consider the equilibrium of a pile with an inclined free surface. However, this problem is still too intricate to be treated as a whole. The second part will then be devoted to determining the stability and the instability of a slice of material at a given distance h from the free surface and parallel to this free surface. We will see that the stability of this slice will depend not only on the angle Θ of the free surface but also on the density of the slice through a parameter P_u. Furthermore, we will see that when the slice is dense enough and when its inclination has reached the limit of stability of the slice, this one will no longer be stable since its inclination has to decrease of a finite quantity $\delta\theta$. We will then relate $\delta\theta$ to the avalanche size and to the avalanche duration D. The third part will be devoted to discussing what occurs for another slice at a different depth h and demonstrating that noise may enhance instabilities of the slice at small h.

1. *Granta gravel assumptions*

According to the Granta gravel model,[17] the grains are rigid, the sample strains are due to plastic yielding only, and the energy losses are governed by a unique friction coefficient $\tan\Phi$, which is independent of the material specific volume. The sample might exhibit dilatancy,[6,8] but it reaches asymptotically the so-called critical state of soil at large plastic yielding. The existence of this critical state, which is only a characteristic state, is a major result of many experimental studies using the triaxial cell technique on soil and sand[16–19] (cf. Sec. IV B). It is also a major hypothesis in this theory. This critical state is characterized by its specific volume v_c. v_c is independent of the material history but depends on the pressure p (i.e., mean stress). We will assume that there is a one-to-one correspondence between p and v_c (i.e., bijection). The reason for this hypothesis will only appear in part (3) of this section. This critical state will be assumed isotropic for the sake of simplicity. The specific volume v of the initial packing may be of course different from the critical-state one v_c.

2. *Statics and dynamics of a slice of material*

Consider now a pile with a constant specific volume v and a flat free surface inclined at an angle Θ to the horizontal plane as is sketched in Fig. 14. There is a plane (labeled PLANE in the figure) parallel to and at a distance h from the free surface. This defines a slice of material that lies on the plane. P and Q are the forces perpendicular and parallel to the free surface which are applied by the slice of material to the plane (or to the bottom part of the pile). Positive directions for P and Q will be downwards. P and Q will then always be positive.

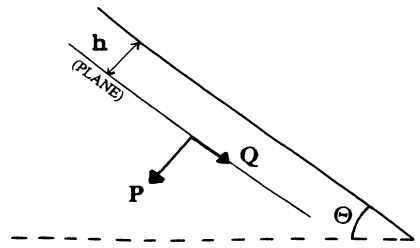

FIG. 14. Sketch of a pile with a free surface inclined at an angle Θ to the horizontal plane. The forces P and Q are applied to the bottom part of the pile by the slice of material delimited by the plane parallel to the free surface and this free surface.

Consider now a slight variation δP and δQ of P and Q. We will consider that δP and δQ are independent and that the pile is near yielding. Therefore, one can assume that δP and δQ induce a small yielding which we will characterize by a volume change $\delta\varepsilon_V$, equivalent to an upward displacement, and a small sliding $\delta\varepsilon_Q$ parallel to the plane; both are localized near the plane. We chose positive $\delta\varepsilon_V$ as volume contractions and positive $\delta\varepsilon_Q$ as downhill slidings; negative $\delta\varepsilon_V$ will then indicate dialatancy. So, according to the plasticity theory, any plastic yielding has to obey a criterion of stability which states that no yielding occurs if

$$\delta P\,\delta\varepsilon_V+\delta Q\,\delta\varepsilon_Q\le 0\ . \tag{19a}$$

We assume that during yielding, some energy is lost due to friction so that the law of energy conservation implies

$$P\,\delta\varepsilon_V+Q\,\delta\varepsilon_Q=MP|\delta\varepsilon_Q|\ . \tag{19b}$$

In the case of Eq. (19b), M is the real friction coefficient, as it is usually defined in soil mechanics and it is related to the friction angle Φ through $M=\tan\Phi$;[31] M is assumed to be a constant according to the Granta gravel model.

We will now calculate the yielding curve, that is to say the set of (P_Y,Q_Y) of two forces which brings the slice just at the limit of equilibrium. We will consider a sliding-down case so that $|\delta\varepsilon_Q|=\delta\varepsilon_Q>0$. According to Eq. (19b), one has

$$\delta\varepsilon_V=(M-Q/P)\delta\varepsilon_Q\ . \tag{20}$$

A set (P_Y,Q_Y) which is at the limit of stability will be kept at the limit of stability by a $(\delta P,\delta Q)$ change if the quality of Eq. (19a) is satisfied, so that yielding curve of the slice obeys

$$\delta P\,\delta\varepsilon_V+\delta Q\,\delta\varepsilon_Q=0\ . \tag{21}$$

Replacing $\delta\varepsilon_V$ by Eq. (20) in Eq. (21) and dividing by $\delta\varepsilon_Q$ leads to the differential equation

$$\delta Q_Y=-(M-Q_Y/P_Y)\delta P_Y\ . \tag{22}$$

Equation (22) is similar to Eq. (13) and its integration leads to the family of yield curves, an example of which is sketched in Fig. 12. Its equation is

$$Q_Y/(MP_Y)+\ln(P_Y)=1+\ln(P_u)\ , \tag{23}$$

where $\ln(P_u)+1$ is the constant of integration. We will assume that P_u depends on the specific volume v_c of the critical state of the pile in a monotonic way and that the smaller v_c, the larger P_u. The reason for this choice will only appear in the next paragraph with the interpretation of Eq. (24), but let us first describe the yield curve. The maximum of P_Y is eP_u for $Q_Y=0$ and the maximum of Q_Y is $Q_c=MP_u=MP_Y$ and is obtained for $P_Y=P_u$. We will see that this last point $(P_u,Q_c=MP_u)$ is the critical state, but first let us define $\tan\Theta_B$ by $\tan\Theta_B=Q_Y/P_Y$. $\tan\Theta_B$ plays the part of a pseudofriction coefficient for the yielding point (P_Y,Q_Y). Near the free surface inclined at Θ the ratio Q/P is $\tan\Theta$ so that the angle Θ cannot overpass Θ_B without sliding occurring. Θ_B is the maximum angle of repose for this slice characterized by P_u.

Consider now a slice which is at the limit of sliding. It is characterized by a (P,Q) set which is on the yielding curve (P_Y,Q_Y). Then increase slightly Θ above Θ_B in order to get yielding. Equation (20) lets us predict three different behaviors for the sliding of this slice depending on whether Θ_B is larger than, equal to, or smaller than the friction angle Φ [$M=\tan(\Phi)$]:

$$\delta\varepsilon_V=0 \text{ if } MP_Y=Q_Y \Longrightarrow \text{specific volume is unchanged}\ , \tag{24a}$$

$$\delta\varepsilon_V<0 \text{ if } MP_Y<Q_Y \Longrightarrow \text{slice dilates}\ , \tag{24b}$$

$$\delta\varepsilon_V>0 \text{ if } MP_Y>Q_Y \Longrightarrow \text{slice contracts}\ . \tag{24c}$$

The slice that obeys Eq. (24a) is in the critical state since its volume does not change when yielding occurs. Therefore, $v=v_c$, $M=\tan\Phi$, $Q_c=MP_Y=MP_u$ at sliding and sliding occurs when $\Theta_B=\Phi$.

The slice that obeys Eq. (24b) dilates. It is then denser than the critical state. It is characterized by $Q_Y/P_Y=\tan\Theta_B>M$ and $\Theta_B>\Phi$. It will be called strong at yield since it will only yield for Θ larger than Φ.

The slice that obeys Eq. (24c) contracts. It is then less dense than the critical state. It is characterized by $Q_Y/P_Y<M$ and yields at an angle Θ_B smaller than Φ. It will then be called weak at yield. However, when the slice yields, densification of the material occurs so that P_u increases and the pseudofriction angle Θ_B increases too. The material then becomes stronger as time goes on. Therefore, the slice will stop yielding spontaneously.

On the contrary, consider a slice that is strong at yield (i.e., with $\Theta_B>\Phi$). It will begin yielding only when $\Theta=\Theta_B$, but, it will dilate when yielding occurs according to Eq. (20) so that its P_u and then Θ_B decreases as the time goes on. The slice cannot stop sliding and an avalanche is created. Yielding will only stop if the angle Θ of the free surface is tilted quickly to a value smaller than the new Θ_B, otherwise this theory predicts the occurrence of a macroscopic event which will only end when the slope reaches a value smaller than Φ. Taking into account the length L of this slope, the size of the macroscopic event is predicted to scale as

$$L^2(\Theta_B-\Phi)l/4\ , \tag{25a}$$

where l is the transverse size of the free surface.

So, according to this critical-state approach, we expect that the avalanche is a macroscopic plastic yielding governed by friction forces and controlled by the sliding of a typical layer inclined at an angle Θ_B. Θ_B exceeds the friction angle Φ. This leads to evaluation of the duration D of the avalanche as the time required to get this slice having slided over a distance L. So, one expects D to obey

$$D=A[L/(2g)]^{1/2}\ , \tag{25b}$$

with

$$A=2\cos^{1/2}(\Phi)/\sin^{1/2}(\Theta_B-\Phi)\ , \tag{25c}$$

where g is the gravity.

Indeed, Eq. (25b) is Eq. (5) of Sec. III. As Eq. (5) corresponds to the experimental law of the avalanche durations, we get a rather good agreement between this theory and the experimental data. Furthermore, consider the rotating drum device which we used in Secs. II and III. It generates avalanches that are stopped partly by collisions with the drum wall and partly due to bead-bead friction so that one may consider that the angle Θ_E of the free surface at which the avalanche stops lies in the range of $\Phi\geq\Theta_E\geq 2^*\Phi-\Theta_B$. So, one may evaluate the experimental values of $\Theta_B-\Phi$ to lie between 1.2° and 2.5°. In turn, this implies that A lies between 9 and 13. These values compare rather well with the experimental measure of A ($A=17$) [see Sec. III, Eq. (5)]. The experimental durations D are slightly longer than the theoretical ones as it is expected since our theoretical approach has not taken into account any building time which would have enlarged the theoretical prediction. Furthermore, this plastic yielding approach predicts an avalanche duration which is independent of the bead size and of the drum length l as we have experimentally observed. At last, this model contradicts the theoretical approach of Jaëger *et al.*[15] where dissipation has been assumed to obey a fluidlike viscosity.

So, we have established Eq. (24) by taking into account (i) friction losses which are characterized by a unique friction coefficient M, (ii) dilatancy effects, and (iii) the existence of the so-called critical state defined by its specific volume v_c and toward which a system evolves asymptotically. In turn, Eq. (24) predicts the existence of macrosocpic avalanches, the size of which scales as the pile volume, when the pile is denser than its critical state and when the free surface is inclined continuously.

We want to finish this part by summarizing these behaviors in the manner used by soil-mechanics specialists and reported in Figs. 11 and 13. Assume then that one is able to control the slope Θ of the pile in such a way that the slice of pile is kept at its limit of yielding. One may then draw the variations of $Q_Y/P_Y=\tan(\Theta_B)$ and ε_V as functions of ε_Q for a given specific volume v. (Such an experiment is not difficult to perform when $v>v_c$, but requires us to decrease quickly Θ when Θ reaches Θ_B when $v<v_c$, otherwise the avalanche will start.) Performing

such an experiment will lead to curves similar to those sketched in Fig. 13.

When $v < v_c$, ε_V and $\tan(\Theta_B) = Q_Y/P_Y$ decrease continuously with time since the pile slice continues dilating and softening. Θ_B and v tend, respectively, to Φ and v_c at long time.

When $v > v_c$, ε_V and $\tan(\Theta_B) = Q_Y/P_Y$ increase continuously with time since the slice of pile continues contracting and hardening; Θ_B and v tend, respectively, to Φ and v_c at long time.

When $v = v_c$, ε_V and $\tan(\Theta_B) = Q_Y/P_Y = \Phi$ are kept constant, independent of time since the slice of pile is in its critical state.

3. *Influence of the depth h on the slice stability*

As we have already mentioned, it has been experimentally observed that the specific volume v_c of the critical state depends on P.[16–19] Moreover, one assumes in general that the critical state obeys the law[17] given by Eq. (10), at large P (Ref. 17) (cf. Sec. IV C):

$$Q_c = MP \ , \tag{10a'}$$

$$v_c = \Gamma - \mu \ln(P) \ . \tag{10b'}$$

However, Eq. (10b) cannot hold near a free surface where P tends to 0 and where we expect v_c to tend to a finite value v_{c0} as found experimentally by Onoda and Liniger.[32] But it is still expected that v_c decreases slightly when increasing P, near $P=0$. So one is led to replace Eq. (10b) by a new equation at small P:

$$v_c = v_{c0} + f(P) \ , \tag{10b''}$$

where $f(P)$ is a function which tends to 0 when P tends to 0.

But a new problem arises. Consider now a homogeneous pile that is strong at yield, with an inclined free surface characterized by Θ and exhibiting a constant density k and a constant specific volume v. Consider also different parallel slices characterized by different thicknesses h. They exhibit the same Q/P value but different values of P according to

$$P = kgh \cos(\Theta) \ , \tag{26}$$

where P is defined for a unit area of the plane and of the slice. Thus, P depends on the slice height h according to Eq. (26), and the specific volume v_c of the "critical" state depends on P according to Eqs. (10b') or (10b''). Therefore, the deeper the slice, the smaller its critical specific volume v_c. This means that the deeper the slice, the nearer from its critical state it is, so the maximum angle of repose Θ_B is smaller at large h than for slices near the free surface. A question arises then:[21,22] why do we observe surface avalanches rather than deep slidings?

There are different possible explanations. The first explanation involves returning to the hypothesis and assuming that a real pile that exhibits avalanches is not homogeneous. Its density increases with depth, so that $\Theta_B(h)$ increases with h.

The second type of explanation may make use of the experimental observation of Reynolds,[6] who discovered that the dilatancy effect is less important near a flat free surface than inside a pile itself. v_c could exhibit a discontinuity at the interface so that the free surface would be characterized by a larger v_c and would be more unstable than the inner part of the pile. This explanation could be supported by the experimental result of Habib[21] who has reported that tilting a sandpile leads to an avalanche when the sand is noncohesive, but that tilting the same noncohesive sandpile leads to landslides when a tiny amount of water is sprayed on the free surface and makes it cohesive.[21]

However, it seems to us that another plausible explanation is based on a noise analysis. Let us assume that one grain in the pile becomes unstable and loses some potential energy E_p. An order of magnitude of E_p is

$$E_p = kgd^4 \ , \tag{27}$$

where d is the grain size. E_P has to be dissipated inside the pile and creates a small dilatation $\delta\varepsilon_V$ localized on a surface S proportional to h^2 ($S = S_0 h^2$). An order of magnitude of $\delta\varepsilon_V$ is then $\delta\varepsilon_V = E_p/(PS)$. Combining this estimate of $\delta\varepsilon_V$ with Eqs. (26) and (27), one gets

$$\delta\varepsilon_V = (d/h)^4/S_0 \ . \tag{28}$$

This means that $\delta\varepsilon_V$ depends drastically on h and the nearer from the free surface the grain is, the larger $\delta\varepsilon_V$ is. This fluctuation process could then enhance the creation of avalanches at the free surface.

Other reasons could also be invoked. For instance, the effect of a slight grain elasticity may be important at high pressure and high pile height.[33,34]

B. The Granta gravel critical-state approach towards self-organized criticality

Let us come back to the discussion of the problem of the avalanche size in a finite pile. It is clear from what has been said in the preceding section that one may observe an avalanche rolling down at the free surface of a pile when tilting the pile. This requires at least that the specific volume v of this pile is denser than the specific volume v_c of the "critical" state everywhere and that the weaker part of the pile stands near the free surface. One then gets a macroscopic event, the volume of which scales as $L^2 l(\Theta_B - \Phi)/4$, with $\Theta_B - \Phi \approx v_c - v$. This event scales then as the pile volume $L^2 l \sin\Phi/2$ and releases a huge amount of potential energy. This scaling implies then a first-order transition problem. (This has already been suggested by Jaëger, Liu, and Nagel[5] on the basis of the difference between the initial and final slopes.)

We know also from soil-mechanics theory that the dilatancy effect of the Granta gravel model could have been taken into account by the introduction of some cohesion σ between grains: σ is positive ($\sigma = \sigma_0$) for grains at rest in a state strong at yield and $\sigma = 0$ when the critical state is reached. This is analogous to an avalanche with a first-order transition, since abruptly releasing σ from σ_0 to 0 when the avalanche occurs abruptly releases an amount of energy E. This is analogous to a latent heat of

transition, since this process is equivalent to unglueing the grains.

This analogy may even be sketched from another point of view: the pile which is flowing down is in its "critical" state, so that yielding (or flow) occurs at a constant volume. In turn, this implies a Poisson coefficient equal to 0.5 which is the Poisson coefficient of a perfect liquid, but before the avalanche occurs the pile has to dilate and its Poisson coefficient differs from 0.5. So, the energy E corresponding to the grain decohesion process of the last paragraph may be viewed as a true latent heat of fusion.

Let us now come to the avalanche problem of a pile in its critical state. Its free surface slides exactly at $\Theta_B=\Phi$ and the energy E needed for grain decohesion is 0. So, the transition between sliding and not sliding will become second order. This pile may perhaps obey the scaling law of the BTW model[9–14] and the avalanche size may exhibit critical fluctuations. Indeed, critical fluctuations have already been observed in finite piles,[29] where $\Theta_B-\Phi$ may be considered as 0 within the experimental uncertainty due to the finite-size effect, as we have discussed in Sec. III E. It seems then to us that a sandpile-avalanche process is similar to a liquid-gas transition which occurs at a given pressure P for a given temperature T. This liquid-gas transition exhibits a latent heat of liquefaction E_L in most cases. However, a critical temperature T_c exists at which $E_L=0$ and where the transition is second order. So, it is tempting to draw an analogy between the sandpile yielding and this liquid-gas transition: $v\leftrightarrow T$ and $v_c\leftrightarrow T_c$. It is worth trying to consider the critical state of Granta gravel for the yielding problem as a true critical point of a phase-transition model.

Thus, we think self-organized critical behaviors may be observed in sandpile avalanches under a few restrictive conditions among which one finds that precise control of the surface and volume densities is required in order to keep the pile surface in the "critical" state and the pile volume at a specific volume smaller than the "critical" specific volume. In such a case, the surface will look like a fluid when $\Theta=\Theta_B=\Phi$ and the continuous model of Hwa and Kardar[14] may describe the flow. However, this is probably not the only requirement and much more work remains to be done in order to precisely define the observation range of the BTW model. For instance, it is not still perfectly clear to us that the macroscopic approach based on a 3D continuous medium, which obeys plastic yielding and assumes that the topology of each neighborhood is invariant with time, is strictly compatible with a sliding process of one grain after one grain as it is assumed in the BTW model.

C. Scaling effects: deep slidings, landslides, macroscopic avalanches, and $1/f$ noise

In Sec. V A, we have seen that a high pile may have its deeper part weaker at yield than its part standing near the free surface. So, there are different ways in which a pile may slide in order to restore its equilibrium. We discuss briefly a few of these processes on the basis of energetic meanings.

For instance, we have sketched three ways in Fig. 15.

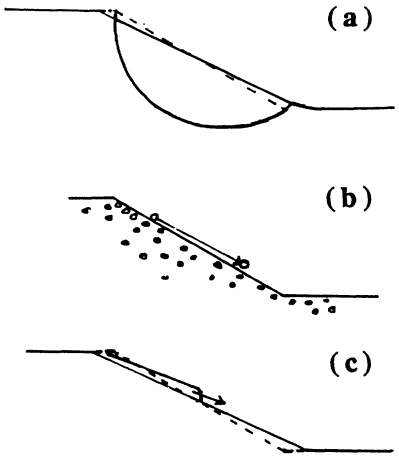

FIG. 15. Different kinds of slidings: (a) deep sliding for which the yielding is localized along a surface at a depth H proportional to the pile size, (b) grain-after-grain sliding as in the BTW model, $\Theta_B\approx\Phi$ ($L\delta\Theta<d$), and (c) macroscopic avalanches characterized by a slope Θ_B larger than the friction angle Φ. The sliding occurs along the slope over a thickness of few or many layers ($L\delta\Theta>d$).

Let us assume that the pile restructures itself so that it restores the angle of repose of its free surface from an angle Θ_B larger than the friction angle Φ to an angle Θ_E lower than Φ. Let us also call $\delta\Theta$ the difference $\Theta_B-\Theta_E$. During this process, the pile loses some potential energy E_p; E_p is dissipated in the pile during the plastic yielding due to friction work E_f, so that $E_p=E_f$ when the equilibrium is restored. Let us assume that $\delta\Theta$ is small and let us call L the length of the pile slope and l its transverse length. H, k, and g will be, respectively, the pile height [$H\approx L\sin(\Phi)$], the pile density, and the gravity. The loss of potential energy is then

$$E_p=gklHL^2\delta\Theta/6\ . \tag{29}$$

We now turn to evaluate the friction loss in the three different cases. We will consider that these losses always obey an intergrain solid friction law governed by a friction coefficient M, as we have assumed so far in this paper.

The first process [Fig. 15(a)] concerns the deep sliding of the upper part of the pile on a sliding surface[35] which is located deep into the pile. Some controversy exists in the real thickness of the yield surface, but the value of this thickness does not enter into the final result of the friction losses as long as this width is much smaller than the depth H at which sliding occurs. As in Fig. 15(a), the typical depth H is approximately the length L of the slope; the typical weight P this surface is bearing is $P=kgHLl/2$. This value of P allows us to estimate that the friction loss to the product of the friction force is $\approx MP$ by the sliding length ϵ is $\epsilon\approx L\delta\Theta$. So E_f is

$$E_f=\beta MgklHL^2\delta\Theta\ , \tag{30a}$$

where β is a numerical factor which depends on the real

geometry of the sliding surface. We see that Eqs. (29) and (30a) are similar. We may then conclude that such a sliding is always possible as far as L is large enough.

In the second sliding process, we consider individual grains sliding along the free surface as it is assumed in the BTW model, but we do not consider any size fluctuation. In this case, each grain of mass m slides along an average distance ϵ which is $\epsilon=2L/3$; it loses a friction energy of $\approx 2\sin(\Phi)gmL/3$. As the number N_0 of grains which have to slide is $N_0=klL^2\delta\Theta/(4m)$ and as $H\approx L\sin(\Phi)$, the energy dissipation due to friction losses is

$$E_f \approx gklHL^2\delta\Theta/6 \ . \tag{30b}$$

Obviously, Eq. (30b) is also equal to Eq. (29) so that this process is always allowed energetically, without any restriction on the pile size.

Let us now study the last process sketch in Fig. 15(c). It is an event that looks like an avalanche. Beads are flowing together at the free surface, but due to the large length L of the slope and to the finite value of $\delta\Theta$, this flow concerns more than one bead layer (since the diameter d of the grain is $d<L\delta\Theta$). In order to estimate the energy losses due to friction, let us try to perform a mean-field approximation. Thus the average pressure $\langle P\rangle$ inside the sliding layer is $\langle P\rangle\approx kgL\delta\Theta/4\cos(\Phi)$. Let us also call $\langle\epsilon\rangle$ the mean displacement of each grain compared to the others. So, the mean friction work per grain is about $\beta' M\langle P\rangle\langle\epsilon\rangle d^2$, with β' some adjustable coefficient. As there are about $L^2\delta\Theta l/(4d^3)$ grains which are sliding, the mean-field approximation leads to a friction energy E_f:

$$E_f \approx \beta' Mkgl L^3\delta\Theta^2\langle\epsilon\rangle/(4d) \ . \tag{30c}$$

Equating Eqs. (29) and (30c) leads to a finite value of $\langle\epsilon\rangle\approx d/\delta\Theta$. This is only possible if $L>\langle\epsilon\rangle$, which requires either a minimum length L (and then a minimum size $d^2l/\delta\Theta$ of avalanches), or large enough $\delta\Theta$ values. This was not the case for processes (30a) and (30b), where the friction dissipation could be large enough whatever the value of $\delta\Theta$. Another interesting point brought about by our mean-field approach of process (30c) is the existence of a finite mean displacement $\langle\epsilon\rangle$ of each grain compared to the others when L is large. This implies that grains which are sliding remain in the same neighborhood as time goes on. In turn, this is a way to confirm the plastic yielding process and this disagrees with the hypothesis of a Brownian motion of grains. The specific behavior of process (30c) is brought about by the existence of a thick sliding zone which couples together the two friction losses of processes (30a) and (30b). In (30a) the losses are generated by small displacements of the sliding zone submitted to high stress P, while they are induced by large displacements of areas submitted to very low stresses in (30b). It is then likely that our mean-field approach of process (30c) hides large variations of grain motion ϵ and stress P: large ϵ will more likely occur near the free surface and vice versa, and small ϵ will be located deeper in the pile.

VI. CONCLUSION

We have used a drum partly filled with glass spheres and rotating slowly around its horizontal axis to study the stability of the inclined free surface of a sandpile and the problem of avalanches. For instance, we have determined the statistics of the avalanche durations D and of the avalanche size $\delta\Theta$ as functions of the sphere diameter d and of the rotation speed Ω of the drum. We have demonstrated that these statistics are rather broad and independent of the parameters Ω and d, for drums that are long enough. They may then be characterized by a mean duration $\langle D\rangle=1.5$ s and a mean avalanche size $\langle\delta\Theta\rangle=2.5°$, which is the difference between the angles Θ_B and Θ_E at which the avalanche starts and stops. We have then found that the flow motion is neither perfectly periodic nor exhibits $1/f$ noise, since the statistics are broad but do not show any long tail. We have also concluded that the avalanche dynamics is governed by inertia and that the avalanche size scales as does the pile size since it is really defined by $\delta\Theta=\Theta_B-\Theta_E$. This last point means that avalanches are really macroscopic events. We have then demonstrated the existence of a change between a 2D avalanche process and a 3D one by studying the avalanche statistics as a function of the number of transverse layers flowing down in parallel at the free surface of the pile (this last parameter is given by the ratio $x=l/d$ of the drum length to the sphere diameter). The crossover occurs at a small value of x, $x_c=4$ so that this phenomenon is likely induced by a change of packing characteristics which involves an order-to-disorder transition. At last, we discuss the existence of different finite-size effects. Especially, we argue that the slope length L has to be larger than the ratio $d/\delta\Theta$ of the sphere diameter divided by the avalanche size if one does not want to observe a finite-size effect which may be responsible for the $1/f$ noise reported in a recent paper.[29] We have then tried to interpret these results within a scheme coherent with other soil mechanics results.

We recalled some classical experimental results on drained noncohesive sand, obtained with a triaxial cell by soil-mechanics specialists. (The tests consist of applying different loads on the top of a cylindrical sandpile maintained in a plastic bag at a given "hydrostatic" pressure and measuring the strains induced by the loading weights.) The results clearly demonstrate a dilatancy effect which is responsible for nonlinear responses such as localizations of yieldings. They also clearly demonstrate the existence of a characteristic state, which is called the "critical" state by soil-mechanics specialists. This state of soil is always reached at large yielding; it is characterized by a unique friction coefficient which is characterized by a coefficient M. M has been found to depend on the soil nature, but not to depend on the value of the mean stress p (i.e., $p\approx$ pressure). The critical state is also characterized by its specific volume v_c which depends on p.

We give then a model of noncohesive soil, the so-called Granta gravel model of Schofield and Wroth,[17] which exhibits the main features of the experimental data. This

model assumes (i) that strains are due to plastic yielding and are governed by plasticity theory, it postulates (ii) the existence of a critical state which is always reached at large yielding in accordance with the experimental evidence and which is characterized by a specific volume v_c, it assumes (iii) that the material may expand or contract during yielding depending on whether it is initially denser or looser than the critical state, and (iv) that energy losses are uniquely due to friction during yielding. This friction is taken into account by introducing (v) a unique macroscopic coefficient M independent of the mean stress p (M is related to the macroscopic friction coefficient $\tan\Phi$ according to Refs. 1, 17, and 31, where Φ is the friction angle). At last, the material is assumed (vi) to be isotropic and the density of the critical state to depend in an explicit way on the mean stress p, cf. Eq. (10).

The main features of this model may be summed up in two different ways. First, the effect of dilatancy may be taken into account by introducing some cohesion (or glue) between the grains of a packing initially denser than the critical state density. The amount of cohesion which has to be introduced depends on the difference between the two densities. The second way consists in introducing a pseudostatic coefficient M' governing the friction losses which is different from the true (i.e., unique) one M and which depends on the specific volume v of the real pile compared to the critical state one v_c. M' is smaller than M for a material looser than the "critical" state and M' is larger than M when the material is initially denser than the critical state.

So, a material which is initially denser than its critical state is called strong at yield since it may undergo stronger shearing than its true coefficient M may allow. However, when yielding starts in such a dense material, it is combined with a dilatation of the material so that this one becomes weaker and weaker as time goes on (the pseudo-M' diminishes) and so that the material ends broken. On the other hand, materials looser than the "critical" state yields for shearing forces less than the predicted values (since $M'<M$). However, this shearing leads to densify the pile. This one then becomes stronger as time goes on and yielding stops spontaneously if the shearing force does not exceed the value predicted with M.

So, it seems to us that the model of Schofield and Wroth links together the two main features of granular materials since it mixes in a unified and combined scheme the effects of solid friction and of dilatancy. These two properties have been discovered by Coulomb[2] and Reynolds.[6]

However, the formal theory of Schofield and Wroth, as explained in Sec. IV, may look a little too intricate and since it is based on the analysis of a triaxial test problem. Such a test is analogous to a bulldozing problem with a loaded pile and is a more intricate case[2] than the stability of a free surface. The slope of the yielding surface of a bulldozed pile may take two different values depending on whether the pile is going up or down. This is why we have derived in Sec. V a simpler version of the Schofield and Wroth theory,[17] which is specially adapted to the avalanche problem. Nevertheless, this theory reaches the same conclusions that are summed up in the last paragraph. Our interpretation of the avalanche process is based on the following scheme. We take a pile with an inclined free surface (angle Θ), which is initially dense enough so that it is initially strong at yield. Consider the problem of the stability of the free surface for which M is equal to the friction coefficient $\tan(\Phi)$. The pile is then characterized by a pseudostatic friction coefficient $M'=\tan(\Theta_B)$ larger than the real one $M=\tan(\Phi)$, which governs the energy losses. So, the pile is stable as far as its slope is smaller than Θ_B. When the slope Θ reaches $\Theta_B>\Phi$, the free surface becomes yielding and dilating, so that M' keeps on decreasing until it reaches M and the free surface instability increases. Flow of beads occurs and cannot stop until the slope Θ of the free surface becomes smaller than Φ and until the potential energy is completely dissipated. This leads to an ending slope Θ_E which lies between Φ and $2\Phi-\Theta_B$. The avalanche is then a macroscopic event whose size $L^2l\delta\Theta$ scales as does the pile size and where $\delta\Theta=\Theta_B-\Theta_E$ lies between $\Theta_B-\Phi$ and $2(\Theta_B-\Phi)$. This scaling has actually been observed.

At the end of the avalanche process, some dissipated energy is used to compact the underlaying pile. Furthermore, this compactness is increased by the natural rotation of the drum which brings, alternatively, the top part at the bottom and vice versa, the bottom at the top. This bottom part experiences "high" pressure corresponding to the weight of the upper part and is compacted. After that, it will become the upper layer. So, these two processes of compaction bring the upper layer of the sample to a density larger than the critical density and explain why the pile is strong at yield.

So, we expect that the avalanche is a macroscopic plastic yielding governed by friction forces and controlled by the sliding of a typical layer inclined at an angle Θ_B larger than the friction angle Φ. This allows us to predict a dynamics controlled by inertia, friction, and gravity and given approximately by Eq. (25). This equation has been experimentally observed [cf. Eq. (5)]. Furthermore, this plastic sliding approach predicts that the avalanche duration D is independent of the bead size and of the drum thickness as it has also been experimentally observed.

As a conclusion of this experimental investigation, it seems to us that coupling the interpretation of avalanche results and those on triaxial cells is possible. This allows us to use a simple model based on the "critical" state of soil mechanics and on a plastic yielding controlled by a unique friction to understand first the existence of catastrophic events (i.e., the bead avalanches) and second their dynamics.

Furthermore, the so-called "critical-state" theory of a granular material allows us to relate the size of these avalanches to the density of the pile at the free surface. It also considers the pile density as a free parameter which may be controlled and adjusted. This may be important, since diminishing the pile density will diminish the avalanche size, so that this may tend to 0. If this state is achieved, the energy stored in the pile and released when the avalanche happens will tend to 0 too, so that the transition between the two states (before and

after the avalanche) may become a second-order transition instead of a first-order one. This tends then to prove that self-organized criticality of avalanche flow may exist. It will only require control of the pile density. These features have allowed us to draw a parallel between the liquid-gas transition, which is most often a first-order transition, but which becomes second-order at $T=T_c$, and the avalanche physics which may exhibit critical behaviors in the meaning of phase transition when the pile has reached its "critical" state in soil-mechanics terms. Recent results on $1/f$ noise generated by finite and small piles seem to confirm our analysis.

However, it seems to us that much work remains to be done in order to confirm our forecasts and to elucidate the true physics of sandpiles. For instance, a large effort is still needed to understand completely the process of strain localization on yield surfaces.[21–24,33,35] A very important parameter in most experimental cases is gravity. It is the true controlling parameter of the compacting process of the granular sample with a free surface.[33,34] One will necessarily have to make it vary. This may be done in three different ways: one may increase gravity using large centrifuge, or diminish it by either using Archimede force and injecting a liquid inside the pores as in the Onoda and Liniger experiments,[32] or by using real gravity-free experiments and free falling in a mine shaft, or even the space shuttle. It seems to us that a gravity-free experiment based on Archimede pressure is highly difficult to perform and control in view of classical, experimental, and theoretical results in soil mechanics.[17] This is why centrifuge experiments are now in process.

As a final comment, we would like to emphasize that the Granta gravel model of Schofield and Wroth, which has been applied here and which takes into account the effect of dilatancy, also predicts nonlinear behaviors and strain localization in triaxial cells, due to the abrupt change of the friction coefficient when macroscopic yieldings occur. It is then very similar to what one may observe for the mechanics of earthquakes[36,37] and of continental tectonics.[38–40] In particular, this model may bring a real physical meaning to the stick-slip earthquake model.[36]

ACKNOWLEDGMENTS

This work could not have been done without the benefit of the numerous interesting and fruitful discussions with soil-mechanics specialists. Professor P. Habib, Professor J. Biarez, Professor J. Salencon, Professor A. Zaoui, Dr. M. Luong, Dr. P.-Y. Hicher, and Dr. J. Desrues are gratefully thanked for their kind advice. We also want especially to thank Professor P. G. de Gennes for the interest he showed in this work and for his stimulating discussions and advice. Professor S. Fauve is greatly thanked for communicating his experimental work prior to publication. The Laboratoire des Matériaux et Structures de Génie Civil is a Unité Mixte No. UMR 113 of the Laboratoire Central des Ponts et Chaussées and the Centre National de Recherche Scientifique.

*Permanent address: Laboratoire O.M.C., Université Paris VI, France.

[1]R. L. Brown and J. C. Richards, *Principles of Powder Mechanics* (Pergamon, Oxford, 1966).

[2]C.-A. de Coulomb, *Mémoires de Mathématiques et de Physique Présentes à l'Académie Royale des Sciences par divers Savans et Lus dans les Assemblées* (L'Imprimerie Royale, Paris, 1773), p. 343.

[3]P. Evesque and J. Rajchenbach, C. R. Acad. Sci. (Paris) **307**, Série II, 223 (1988).

[4]P. Evesque and J. Rajchenbach, *Powders and Grains,* edited by J. Biarez and R. Gourvès (Balkema, Rotterdam, 1989), pp. 217–224.

[5]H. M. Jaëger, C.-H. Liu, and S. Nagel, Phys. Rev. Lett. **62**, 40 (1989).

[6]O. Reynolds, Philos. Mag. **20**, 469 (1885).

[7]R. A. Bagnold, Proc. R. Soc. London Ser. A **225**, 49 (1954).

[8]R. A. Bagnold, Proc. R. Soc. London Ser. A **295**, 219 (1966).

[9]P. Bak, C. Tang, and K. Wiesenfeld, Phys. Rev. Lett. **59**, 381 (1987).

[10]P. Bak, C. Tang, and K. Wiesenfeld, Phys. Rev. A **38**, 364 (1988).

[11]C. Tang and P. Bak, Phys. Rev. Lett. **60**, 2347 (1989).

[12]L. P. Kadanoff, S. R. Nagel, L. Wu, and S.-M. Zhou, Phys. Rev. A **39**, 6524 (1989).

[13]D. Dhar and R. Ramaswamy, Phys. Rev. Lett. **63**, 1659 (1989).

[14]T. Hwa and M. Kardar, Phys. Rev. Lett. **62**, 1813 (1989).

[15]H. M. Jaëger, C.-H. Liu, S. R. Nagel, and T. A. Witten, Europhys. Lett. **11**, 619 (1990).

[16]J. Biarez and P. Y. Hicher, *Powders and Grains,* edited by J. Biarez and R. Gourvès (Balkema, Rotterdam, 1989), pp. 1–13.

[17]A. N Schofield and C. P. Wroth, *Critical State of Soil Mechanics* (McGraw-Hill, London, 1968).

[18]M. P. Luong, Geotech. Testing J. **9**, 80 (1986).

[19]M. P. Luong, *Proceedings of the International Symposium on Soil Under Cyclic and Transient Loading* (Balkema, Rotterdam, 1980), p. 315.

[20]M. Oda and T. Sudoo, *Powders and Grains,* edited by J. Biarez and R. Gourvès (Balkema, Rotterdam, 1989), pp. 155–161.

[21]P. Habib, Rev. Fr. Geotech. **31**, 5 (1986).

[22]P. Habib, Rev. Fr. Geotech. **27**, 7 (1984).

[23]J. Desrues, Thèse d'etat, Université de Grenoble, France, 1984.

[24]J. Desrues, J. Lanier, and P. Stutz, Eng. Fract. Mech. **21**, 909 (1985).

[25]D. R. Nelson and F. Spaepen, *Solid State Physics* (Academic, New York, 1989), Vol. 42.

[26]M. Gherbi, R. Gourvès, and M. C. Reymond, *Powders and Grains,* edited by J. Biarez and R. Gourvès (Balkema, Rotterdam, 1989), pp. 129–133.

[27]R. Bidaux, N. Boccara, and H. Chate, Phys. Rev. A **39**, 3094 (1989).

[28]S. Fauve, C. Laroche, and S. Douady, unpublished and private communication.

[29]G. Grinstein *et al.* (unpublished).

[30]For a small history, the Granta gravel model for drained sand (and the Cam clay one for undrained material) were proposed

by the Engineering Department of the University of Cambridge (U.K.); this University is on the Cam river, with a famous bridge that splits the river in upstream and downstream flows; to the best of our knowledge, one of these streams is called Cam and the other Granta and hence the names of these models.

[31]The relationship $M=\tan\Phi$ holds only in the formulation of the sliding problem at a free surface as in Sec. V. This is due to the fact that Q is a shear stress in Sec. V. However, we want to emphasize that this relation $M=\tan\Phi$ does not hold in Secs. IV B and IV C [Eq. (11)], where stresses σ_1 and σ_3 are the maximum and minimum principle stresses of the problem, and are not the maximum shear stresses. In Sec. IV then, these stresses σ_1 and σ_2 are related to the mean stress $p=(\sigma_1+2\sigma_3)/3$ and to the deviatoric stress $q=\sigma_1-\sigma_3$ according to the definitions of Sec. IV A. In Sec. IV also, the maximum shear stress may be calculated as a function of σ_1 and σ_3 (or to p and q) in the case of a triaxial test. A simple way to do so at the limit of stability is to use the Mohr circle method (Ref. 1) so that one gets $\sin\Phi=(\sigma_1-\sigma_3)/(\sigma_1+\sigma_3)=q/(2p+q/3)$. As $M=q/p$ [Eq. (10a)] at large plastic yielding, one finally has $\sin\Phi=3M/(6+M)$ in the case of a triaxial test with cylindrical symmetry. There exists a one-to-one correspondence between Φ and M in the triaxial test case as mentioned in Sec. IV. It is different from $\tan\Phi=M$, however.

[32]G. Y. Onoda and E. G. Liniger, Phys. Rev. Lett. **64**, 2727 (1990).

[33]P. Habib, Rev. Fr. Geotech. **48**, 35 (1989).

[34]F. H. Lee and A. N. Schofield, Geotech. **38**, 45 (1988).

[35]P. Habib, Rev. Fr. Geotech. **34**, 5 (1986).

[36]J. M. Carlson and J. S. Langer, Phys. Rev. A **40**, 6470 (1989).

[37]D. J. Blundell, Contemp. Phys. **22**, 335 (1981).

[38]G. Peltzer, Bull. Geol. Inst. Univ. Uppsala **14**, 115 (1988).

[39]G. Peltzer and P. Tapponnier, J. Geophys. Res. **93**, B12, 15 085 (1988).

[40]A. Sornette and D. Sornette, Europhys. Lett. **9**, 197 (1989).